An Assessment of the State-of-the-art in Multidisciplinary Aeromechanical Analyses

Anubhav Datta
ELORET Corporation
Ames Research Center
Moffett Field, CA
datta@merlin.arc.nasa.gov

Wayne Johnson
Aeromechanics Branch
NASA Ames Research Center
Moffett Field, CA
wayne.johnson@nasa.gov

ABSTRACT

This paper presents a survey of the current state-of-the-art in multidisciplinary aeromechanical analyses which integrate advanced Computational Structural Dynamics (CSD) and Computational Fluid Dynamics (CFD) methods. The application areas to be surveyed include fixed wing aircraft, turbomachinary, and rotary wing aircraft. The objective of the authors in the present paper — together with a companion paper on requirements — is to lay out a path for a High Performance Computing (HPC) based next generation comprehensive rotorcraft analysis. From this survey of the key technologies in other application areas it is possible to identify the critical technology gaps that stem from unique rotorcraft requirements.

INTRODUCTION

This paper presents a survey of computational aeroelasticity in the disciplines of fixed wing aircraft, turbomachinery, and rotary wing aircraft. The work was undertaken by the U.S. Army Aeroflightdynamics Directorate under the High Performance Computing Institute for Advanced Rotorcraft Modeling and Simulation (HI-ARMS) and NASA.

The survey covers the emerging methods which integrate Reynolds-averaged Navier-Stokes (RANS) CFD, Finite Element Method (FEM) based structural mechanics, and high-fidelity coupling procedures designed to satisfy the unique requirements of each discipline. In each discipline, the key aeromechanical phenomena which determine the costs and risks associated with design, but remain beyond current prediction capabilities, are described. The current status of High Performance Computing (HPC) based high-fidelity studies on the key phenomena are reviewed, the recent advances summarized, and the unresolved challenges highlighted.

The central theme of this paper is rotorcraft. The objective of the authors — together with a companion paper on requirements [1] — is to lay out a path for a High Performance Computing (HPC) based truly comprehensive next generation rotorcraft code; comprehensive in solutions (performance, loads, stability, vibration, handling qualities), comprehensive in applications (ground, hover, steady flight, unsteady maneuvers), and comprehensive in scope (arbitrary geometries, innovative configurations). The intention of the present review is to identify the key technologies in other application areas that can be drawn upon to this end, and to identify the critical technology gaps that stem from unique rotary

Presented at the AHS Specialist's Conference on Aeromechanics, San Francisco, CA, January 23-25, 2008.

wing requirements.

The paper is divided into five sections. The first section presents a description of the state-of-the-art in high-fidelity fluid structure coupling. This is followed by three sections, one each on the status of computational aeroelasticity in fixed wing aircraft, turbomachinery, and rotary wing aircraft. Each section is subdivided into two parts; the first part is on structural mechanics, the second part is on coupled fluid-structure applications. The CFD methods applicable to each discipline are not reviewed in this paper. The last section summarizes the different CFD/CSD coupling nomenclatures used in the three disciplines.

FLUID-STRUCTURE COUPLING

Definition of the problem

The problem of fluid-structure coupling involves three issues: (1) temporal accuracy, (2) spatial accuracy, and (3) interface geometry representation. The purpose of the present discussion is to clarify their meaning, explain why they were of little importance in rotorcraft so far, and highlight why they are important now and for the future.

At the PDE level, the three issues are related to the following questions. The first issue, that of temporal accuracy, is related to the question whether two systems of coupled PDEs of different types can be solved separately, one after the other, one step at a time, exchanging solutions at each time step. This is the method of partitioned formulations that begins with an acceptance that fluid PDEs of convection-diffusion type, and structural PDEs of elliptic type are best solved separately in their own domains using their own efficient solvers. The main task then is to devise a method of solution exchange which renders the process at least as time accurate as the worse of the two solvers. The second and the third issues, those of spacial accuracy and interface geometry representation, are related to errors introduced during solution exchange across domains. Depending on these errors the method of solution exchange must be re-constructed to achieve an intended temporal accuracy. Note that the second and the third issues are independent of the first, that is, they arise whether or not a partitioned procedure is adopted.

Partitioned vs. fully coupled formulations

The practical benefits of partitioned formulations are obvious — modularity of framework, and domain separation for refinements. However, an appropriate method of solution exchange must be designed to ensure time accuracy. Fully coupled formulations, on the other hand, are strictly time accurate without this additional burden. However, such formulations require: (1) a common time integrator, and (2) solution of an algebraic system, at each Newton-like step, that includes both fluid and structural stiffness. The second requirement is not easy to meet for the following reasons. Direct solution is not an option, since modern CFD (without the use of reduced order modeling) provides far too many degrees of freedom (DOFs), typically 10-100M for rotorcraft. Iterative solution is the natural option in CFD. The temporal evolution of a convection-diffusion equation is naturally analogous to the iterative convergence of an algebraic system. Moreover, they are easy to parallelize. On the other hand, iterative solvers are traditionally not preferred for structures. The convergence rates of iterative solvers depend on the condition number of the system (for symmetric positive definite matrices the condition number is the ratio of the largest to the smallest eigenvalues, or natural frequencies squared). Typically, aerospace structures pose 4-th order elasticity problems involving bending-torsion-extension of thin beams, or bending-shear-extension of thin plates, and shells. Condition numbers for such structures range from 10^8 to 10^9 (the number for a typical rotor beam model is around 10^9). In comparison, the maximum condition number for a 2-nd order fluid problem can be as high as 10^6. Pre-conditioners that are well suited for structures are not suitable for fluids. For example, the incomplete Cholesky pre-conditioner cannot be applied to fluids as the fluid system is not symmetric positive definite. Similarly, pre-conditioners well suited for fluids, like the block Jacobi (easily parallelizable), can only be used for structures with special re-ordering and sparsity fill-in for reasonable, yet problem dependent, convergence. Moreover, such procedures demonstrate poor scalability. Thus, the challenge of a unified solution procedure in the presence of CFD is real [2].

The difficulty is bypassed for structures that are less ill-conditioned. One example is turbomachinery structures. These are modeled using solid elements, governed by 2-nd order elasticity. Gottfried and Fleeter [3] have used full coupling for turbomachinery aeroelasticity. Their analyses, TAM-ALE3D, a refined version of the original ALE3D code developed in the Lawrence Livermore National Laboratories, is a fully coupled finite element analysis that has been applied to turbomachinery flutter calculations. A second example is biological structures. Here, structures are either membrane-like, or thick, when shell-like. Bathe and Zhang [4] have applied full coupling in biomedical fluid flows, as well as general internal flows in mechanical components. Their analysis is used extensively for biomedical and mechanical applications, as part of the ADINA commercial software code. An option for partitioned formulation is also provided (the authors denote them as direct and iterative proce-

dures). The foundations of all fully coupled approaches can be traced back to the Arbitrary Lagrangian Eulerian (ALE) formulation of conservations laws, first introduced by Hirt et al. [5] in 1974 for fluid flows at all speeds. It was applied by Donea [6] in 1983 for fluid-structure interaction problems. Bendikson [7, 8] first applied this technique in the early 1990s for flutter calculations and demonstrated minimal errors in energy transfer between fluids and structures. Fully coupled formulations are also termed monolithic formulations.

In summary, for aerospace structures, partitioned formulations provide fundamental advantages over fully coupled ones, in addition to their obvious practical benefits.

Current coupling practices in rotorcraft

Classical comprehensive analyses, which use lifting-line or lifting-surface models, involve at the most 1-10K DOFs. The formulation is fully coupled, and is solved using direct methods. Thus the first issue of temporal accuracy is satisfied. To re-iterate, the need for a partitioned formulation for fluids and structures is felt only under the following two circumstances. First, when millions of fluid DOFs call for an iterative solver whereas the structural DOFs, being ill-conditioned, call for a direct solver, or at least a different pre-conditioner. Second, when these conflicting requirements of fluids and structures are very easily met in separate domains. The second issue of spatial accuracy is easily satisfied by such formulations as the structural shape functions are available to the fluid terms. The third issue of interface geometry representation has also been simple, so far, in rotorcraft. This is because the beam theory, or any single component structural model, regardless of 1-D, 2-D, or 3-D, provides a simple yet rigorous definition of the surface. The complexity arises in multi-component structures like the fuselage.

Dynamics researchers have carried out coupled rotor-fuselage analysis, but at a time when CFD airloads were beyond state of the art. With the emergence of this capability, there is a requirement to address the issue of geometry representation. A detailed dynamic model is not necessarily the best suited for fluid-structure coupling. The surface geometry representation is more important than the internal load paths. Thus, the requirement is to have, at the least, a shell model that re-produces the low frequency modes (up to 40 Hz), and at best, a detailed model that includes the outer skin. Fixed-wing researchers have already accomplished these tasks, and there is a volume of literature that can be drawn upon.

Rotorcraft CFD/CSD coupled analyses have used partitioned procedures. The focus so far has been on the rotor. For an isolated rotor, the wetted surface is rigorously defined. The shape functions are available. Thus the issues of spatial accuracy and surface representation are easily dealt with. The issue of temporal accuracy is enforced concurrently with Newton-Raphson type iterations for determining the trim angles. For a time marching solution, the procedure is conceptually simpler as the trim angles are left undetermined, but requires the enforcement of temporal accuracy at every time step. The problem is then the same as that faced by fixed-wing researchers, where it has been of great importance due to the emphasis on flutter. Small errors in coupling result in erroneous energy exchange and affect flutter boundaries adversely. The emphasis in rotors has been on loads. Errors in fluid-structure coupling are less visible. The problem is further compounded in fixed-wing because of its 3-D structure and multiple sub-structures. Without a detailed 3-D structure, this difficulty has not been faced yet in rotorcraft.

Temporal accuracy

The temporal accuracy of partitioned formulations is the main focus of high-fidelity fluid-structure coupling. Physically, it means that the airloads and structural loads at a given time step are consistent with one another. Numerically, it means that the temporal error is driven down to the level of the worse solver.

One effective approach is the use of sub-iterations between every consecutive pair of time steps. The method was first applied in aeroelastic computations by Strganac and Mook [9], followed by Weeratunga and Pramono [10], and more recently by Melville and his co-researchers [11, 12]. The method is time intensive for RANS. Potential innovations may involve the coupling of structural dynamics with the fluid sub-iterations.

Early work in fixed-wing fluid structure coupling involved sub-iteration free, straight-forward time integration. See for example, Edwards [13], Bennet [14], and Guruswamy et al. [15, 16]. In the serial approach, one solver waited for the completion of the other, before exchanging solutions and advancing to the next time step. In the parallel approach, both solvers advanced simultaneously, followed by solution exchange before advancing to the next step. The latter was proposed originally by Weeratunga and Pramono [10], and refined subsequently by Farhat and Lesoinne [17]. The original work involved accompanying sub-iterations due to the relative instability of the scheme. The subsequent refinement improved stability without sub-iterations, at the cost of exchanging solutions twice at each time interval. Since then, a significant amount of research has been conducted on devising sub-iteration free methods that retain, at the least, second-order accuracy. Farhat and his co-researchers [18]

have described the formal design of such methods.

Sub-iteration free approaches are predictor-corrector schemes, tailored to the individual time integrators. A generalized predictor-corrector approach is illustrated below, adopted from the last reference. The mesh deformation is denoted by x, the fluid variables are denoted by q, and the structural deformations by u. The time step is denoted by n. The fluid-structure interface boundary is denoted by Γ. For example u_Γ denotes the structural deformations at the interface, a subset of u. The symbol $\longleftarrow$ denotes a time integrator and shows dependencies on the latest time steps. A single time step advancement is given as follows.

1. Predict deflections for the next time step

$$u_\Gamma^{n+1^P}$$

2. Update mesh points x. Mesh boundary points denoted by x_Γ. Mesh internal points denoted by x_Ω. The boundary mesh points can be updated as

$$x_\Gamma^{n+1^P} \longleftarrow x_\Gamma^{n^P}, u_\Gamma^{n+1^P}$$

For example,

$$x_\Gamma^{n+1^P} = x_\Gamma^{n^P} + \bar{\mathbf{U}}_\Gamma \left(u_\Gamma^{n+1^P} - u_\Gamma^{n^P} \right)$$

The above equation simply represents the discretized deflection and velocity compatibilities on the surface. Without re-griding in time, the deflection compatibility is given by $x = \mathbf{U}_\Gamma u$ where $\mathbf{U}_\Gamma$ is simply the transformation that connects the CFD surface grid to the structural grid. For perfectly matched meshes $\mathbf{U}_\Gamma$ is equal to the identity matrix. The velocity compatibility is $\dot{x} = \mathbf{U}_\Gamma \dot{u}$. If the structure reaches out to the wetted surface, and the shape functions are known, $\mathbf{U}_\Gamma = \mathbf{H}$, where $\mathbf{H}$ are the shape functions. With re-griding, the mesh connectivity changes with time, i.e. the transformation $\mathbf{U}_\Gamma$ is now a function of time, and the discretized velocity compatibility is expressed as $\dot{x} = \bar{\mathbf{U}}_\Gamma \dot{u}$ where $\bar{\mathbf{U}}_\Gamma$ denotes a selected combination of $\mathbf{U}_\Gamma$ over previous time steps, e.g. the mean of $\mathbf{U}_\Gamma^n$ and $\mathbf{U}_\Gamma^{n-1}$.

The internal points are updated based on the boundary points

$$x_\Omega^{n+1^P} \longleftarrow x_\Omega^{n^P}, x_\Gamma^{n+1^P}$$

3. Update fluid solver using updated mesh

$$q^{n+1} \longleftarrow q^n, x^{n+1^P}$$

4. Calculate structural forcing

$$\begin{aligned} F_s^{n+1} &= F_s\left(q^{n+1}, x_\Gamma^{n+1^P}\right) \\ &\text{or} \quad F_s\left(q^n, x_\Gamma^{n^P}\right) \text{... or other forms.} \end{aligned}$$

5. Update structural solver

$$u^{n+1} \longleftarrow u^n, F_s^{n+1} \quad (\text{ including } \; u_\Gamma^{n+1} \;)$$

The predictor is on displacement (step 1). The corrector is on forcing (step 4). Methods of the above type are classified as *loose coupling* in the fixed wing community. If the above procedure is carried out multiple times at the same time step (i.e. sub-iterations), then the following can be enforced

$$u_\Gamma^{n+1^P} = u_\Gamma^{n+1}$$

which implies that the mesh deformation follows

$$x_\Gamma^{n+1} = x_\Gamma^n + \bar{\mathbf{U}}_\Gamma \left(u_\Gamma^{n+1} - u_\Gamma^n \right)$$

rather than

$$x_\Gamma^{n+1^P} = x_\Gamma^{n^P} + \bar{\mathbf{U}}_\Gamma \left(u_\Gamma^{n+1^P} - u_\Gamma^{n^P} \right)$$

and hence enforces the velocity compatibility $\dot{x} = \bar{\mathbf{U}} \dot{u}_\Gamma$ strictly. The forcing and structural response (step 4 and 5) are also consistent, as $x_\Gamma^{n+1^P}$ is replaced with x_Γ^{n+1}. The method with sub-iterations is classified as *close coupling*, *tight coupling*, or *strong coupling* in the fixed wing literature. The force predictor in step 4 can be chosen in various ways. The first form is also called serial staggering. The second form is called parallel staggering, simply because the fluid and structural updates (step 3 and 5) can be performed independently of one another.

The methods that enforce second-order accuracy, without sub-iterations, rely on the formal selection of: (1) the integrators, i.e. the arrows '$\longleftarrow$', (2) the initial predictor, i.e. step 1, and (3) the form of the force corrector, i.e. step 4. Two illustrative examples are provide in reference [18] based on a second-order fluid integrator, and a second-order (Newmark type) structural integrator. Unless formally selected, the sub-iteration free methods provide only first-order accuracy.

Lastly, we note that for non-CFD Lagrangian aerodynamic models, the time iteration procedure is simpler as there are no grid motions. The need to reconcile the Geometric Conservation Law and structural motion update does not arise. The structural forcing F_s is related directly to the deformations u. The serial and parallel staggered schemes along with sub-iterations can be implemented as follows.

1. Serial staggered with sub-iterations

   Predict u^{n+1^P}

   Then, perform successively

   $F_s^{n+1} \longleftarrow F_s^n, u^{n+1^P}$; in step 1

   $u^{n+1} \longleftarrow u^n, F_s^{n+1}$; in step 2

   Iterate until convergence, i.e. $u^{n+1^P} \approx u^{n+1}$

2. Parallel staggered with sub-iterations

   Predict u^{n+1^P}

   Then, perform in a single step

   $F_s^{n+1} \longleftarrow F_s^n, u^{n+1^P}$;

   $u^{n+1} \longleftarrow u^n, F_s^n$;

   Exchange updates, i.e. update u^{n+1^P} with u^{n+1} in the airloads integrator, and update F_s^n with F_s^{n+1} in the structures integrator, and iterate until convergence.

The parallel staggered method is advantageous when the fluid and the structure are run on separate processors. The parallel method has inferior stability and requires requires lower time steps.

Spatial accuracy

Assume that the structural model includes a rigorous interface geometry representation. However, the CFD and the CSD discretizations will not, in general, match at the interface. The deformation and structural forcing must be mapped correctly across the non-matching interface. Generic methods which are 'exact' regardless of the blade shape are critical for the evaluation of advanced geometry blades. Two such methods are formulated below.

Deformation mapping deals with the correct evaluation of $\bar{\mathbf{U}}_\Gamma$ in step 2 (see previous section). Loads transfer deals with the correct evaluation of structural forcing F_s in step 4. The latter implies an exact evaluation of the virtual work term. This is a necessary energy conservation requirement. In addition, it is desirable, though not necessary, that the total integrated forcing be preserved during the mapping.

Deformation mapping is straight-forward when the shape functions are available. Loads transfer can be accomplished via: (1) integrated force coupling, and (2) direct traction coupling. In the integrated force coupling, the virtual work is calculated based on integrated fluid stresses (pressure and skin friction) over a surface patch. In surface traction coupling, the virtual work is calculated based on the pressure and shear distributions directly. The first method preserves total forces, but does not guarantee energy conservation for a finite mesh. The second method is strictly energy conservative, but does not guarantee preservation of total forces. Thus, they are complimentary to each other. However, as long as interpolations and integrations are performed consistently within each domain, both satisfy and conservation and preservation in the limit of mesh refinement.

Both methodologies can be formulated for rotor blades. Simple illustrations are given below.

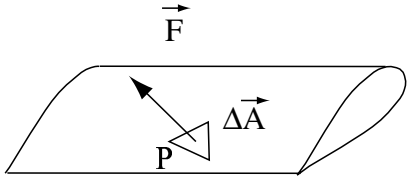

Figure 1: **A concentrated force on a rotor blade obtained by integrating fluid stresses over a surface patch of area $\Delta\vec{A}$**

The integrated force coupling is formulated as follows. Consider a concentrated force $\vec{F}$ acting at a point P on the deformed blade, Fig. 1. $\vec{F}$ is integrated traction over an arbitrary patch of area $\Delta\vec{A}$. The virtual work done by the force is simply

$$\delta W = \vec{F} \cdot \delta\vec{r}_P \tag{1}$$

where $\vec{r}_P$ is the position vector of the point P, and $\delta\vec{r}_P$ is its virtual displacement. The position can be expressed as

$$\vec{r}_P = r^T e^0 \tag{2}$$

r are the scalar components and $e^0 = [ijk]^T$ is a set of unit vectors. Let u be the states of blade deformation. The virtual displacement then becomes

$$\delta\vec{r}_P = (\mathbf{D}\delta u)^T e^0 \tag{3}$$

where $\mathbf{D}$ is the derivative matrix of the scalar components r with respect to the states u. Henceforth, matrices are denoted in bold capital letters. In beam theory, the states are typically three deflections and three rotations $u = [u_1, u_2, u_3, \theta_1, \theta_2, \theta_3]$. $\mathbf{D}$ is then the (3×6) derivative matrix. Expressing the force in the same basis

$$\vec{F} = F^T e^0 \tag{4}$$

gives

$$\delta W = F^T \mathbf{D}\delta u \tag{5}$$

If q are the N generalized nodal displacements of a finite element containing the point P, and $\mathbf{H}$ is the $(6 \times N)$ elemental shape function matrix, it follows from $\delta u = \mathbf{H}\delta q$

$$\delta W = F^T \mathbf{D}\mathbf{H}\delta q = Q^T \delta q \tag{6}$$

The generalized nodal force is then given by

$$Q = \mathbf{H}^T \mathbf{D}^T F \tag{7}$$

The term $\mathbf{D}^T$ transmits the airloads in 3-D space to the 1-D beam structure. The matrix $\mathbf{D}$ varies with the choice of beam theory. Note that, from eqn. 3, the virtual displacement components are

$$\delta r_P = \mathbf{D}\delta u = \mathbf{D}\mathbf{H}\delta q \tag{8}$$

Equations 7 and 8 highlight the well-known relation that the generalized structural forcing vector relate to the aerodynamic forcing via the transpose of the relation that connects the aerodynamic deflections to structural deflections. Here, **DH** can be interpreted as the equivalent elemental shape functions in 3-D space for the corresponding beam theory.

Note that the force method ensures that the total integrated forces (and moments) remain the same when transferred from the fluid to the structural domain. However, because the point of application of $\vec{F}$ within each surface patch is arbitrary, the method is energy conservative only in the limit of mesh refinement. Strict conservation can be enforced using traction coupling.

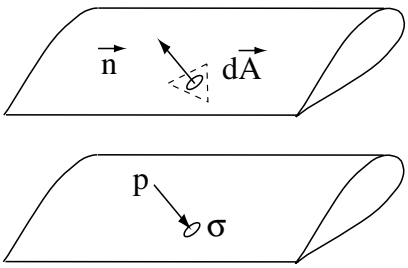

Figure 2: **Fluid pressure and surface shear over a rotor blade differential area** $d\vec{A}$

The direct traction coupling is formulated as follows. Consider a differential area $d\vec{A}$ within the surface patch $\Delta\vec{A}$ of magnitude dA and unit normal $\vec{n}$, Fig. 2.

$$d\vec{A} = \vec{n}dA = n^T e^0 dA \tag{9}$$

The differential force generated by the pressure is

$$-pd\vec{A} = -pn^T e^0 dA$$

The differential force generated by the fluid stress tensor along the direction of $d\vec{A}$ is

$$\sigma_{\mathbf{F}} \cdot d\vec{A} = \sigma_{\mathbf{F}} \cdot \vec{n}dA = (\sigma_{\mathbf{F}} n)^T e^0 dA$$

In the force coupling case, the following integration was performed in the fluid domain.

$$\begin{aligned}\vec{F} &= \int_{\Delta A} -p\, d\vec{A} + \sigma_{\mathbf{F}} \cdot d\vec{A} \\ &= \left[-\int_{\Delta A} p\, n^T\, dA + \int_{\Delta A} (\sigma_{\mathbf{F}} n)^T\, dA \right] e^0 = F^T e^0\end{aligned} \tag{10}$$

The integrated force was then transferred to the structural domain. **H** and **D**, required for this calculation, were available in the structural domain. Now consider the virtual work calculation using fluid traction.

$$\begin{aligned}\delta W &= \int_{\Delta A} \left(-p\, d\vec{A} + \sigma_{\mathbf{F}} \cdot d\vec{A} \right) \cdot \delta\vec{r}_P \\ &= \int_{\Delta A} \left[-p\, n^T + (\sigma_{\mathbf{F}} n)^T \right]\, e^0 \cdot (\mathbf{D}\delta u)^T\, e^0 dA \\ &= \int_{\Delta A} \left[-p\, n^T + (\sigma_{\mathbf{F}} n)^T \right] \mathbf{DH}\delta q dA = Q^T \delta q\end{aligned} \tag{11}$$

The generalized nodal force then becomes

$$Q = \int_{\Delta A} \left[-\mathbf{H}^T \mathbf{D}^T n\, p + \mathbf{H}^T \mathbf{D}^T \sigma_{\mathbf{F}}\, n \right] dA \tag{12}$$

Note that the integration involves variables from both domains. If performed in the fluid domain, exact values of **D** and **H** must be received from the structural domain at the fluid Gauss points. Similarly if performed in the structural domain, exact values of p and $\sigma_{\mathbf{F}}$ must be received from the fluid domain at the structural Gauss points. The value of n is different in both (except in the ideal case when the meshes and spatial orders match exactly). Unlike integrated force coupling, direct traction coupling ensures the exact calculation of virtual work.

There has been significant contributions by various researchers to address the issue of conservation and preservation, within the context of temporal accuracy. See for example, Maman and Farhat [19], Cebral and Lohner [20], Farhat et al. [21], Slone et al [22], and Michler et al. [23]. The key conclusion is that exact conservation and preservation can be ensured in the limit of mesh refinement only when interpolations of all the variables are performed using schemes consistent with their domain. For example, p and σ_F can be interpolated only in the fluid domain and then transferred. Similarly, deformations can be interpolated only in the structural domain and then transferred.

Neither of these methods have been applied to rotorcraft CFD/CSD so far. In the current applications, the rotor blade is excited by force and moment distributions (per span) along its local sectional elastic axis. The force and moment excitations are obtained by integrating the fluid stresses along chord-wise strips. Chord-wise strips are an easy and natural choice for structured grids. The excitations, if calculated at the structural Gauss points along the elastic axis (using interpolation in the fluid domain), or imposed as concentrated forces, one for each strip using the shape functions, would satisfy conservation and preservation requirements in the limit of mesh refinement.

The exact generic methods provide significant advantages over the current methods of sectional airloads. First, the method of sectional airloads is arbitrary for advanced geometry blades, a simple example of which is the BERP tip. For such geometries it is necessary to

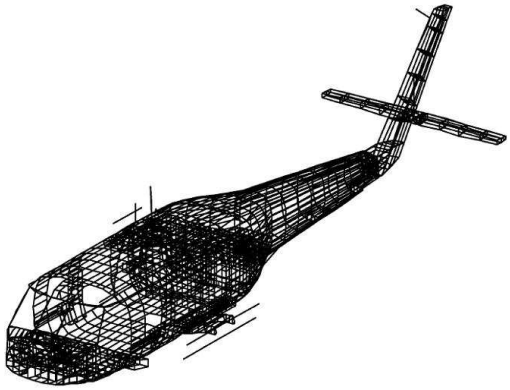

Figure 3: **FEM model (MSC NASTRAN) of a SH-60 Sea Hawk fuselage developed by Sikorsky and used in UMARC rotor-fuselage coupled dynamic analysis; Yang et al. 2004**

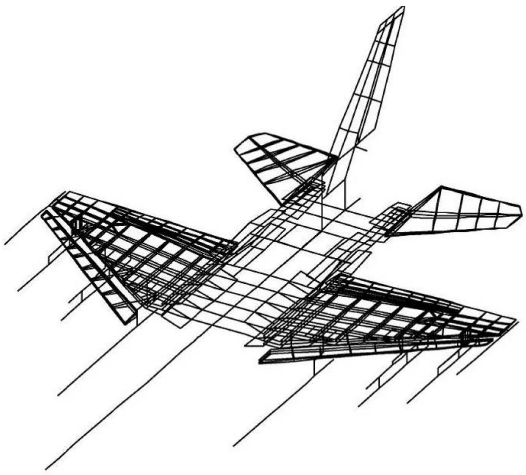

Figure 4: **FEM model of a F-16 fighter used in a doublet-lattice aerodynamic model based typical fixed-wing flutter analysis; Denegri 2005**

use the exact generic methods for high-fidelity coupling. Second, the generic methods are equally applicable for both structured and unstructured grids, the latter being increasingly applied today for near-blade flows. Third, the methods are well-suited for the long term CFD goal of near blade adaptive refinement. Fourth, the generic methods are equally applicable for the rotor, fuselage, and any structure in general, as long as the interface geometry representation is clearly defined.

Interface geometry representation

The issue of interface geometry representation involves the rigorous description of the surface based on the underlying structural model. The method of description differs based on: (1) whether the structural shape functions are available, and (2) even if the shape functions are available whether the structural model reaches out to the wetted surface. The problem posed by the unavailability of shape functions is a practical complication that is ideally avoided. The problem posed by the structure not reaching out to the wetted surface is more fundamental. For a single component structure, e.g. a rotor blade beam model, the necessary interpolation and extrapolations are rigorously defined by the underlying theory (e.g. note the term $\mathbf{D}$ in eqn 7 in addition to $\mathbf{H}$). Complications arise for multiple intersecting sub-structures, as is the case for airframes.

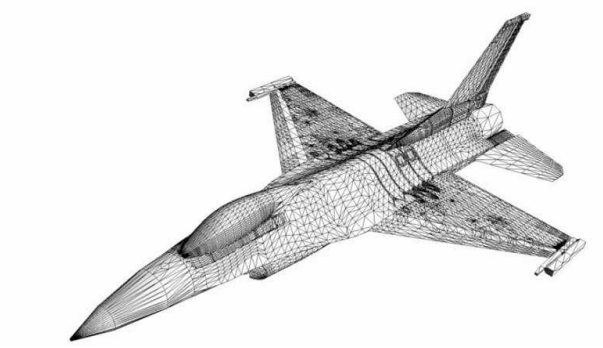

Figure 5: **Detailed FEM model of a F-16 fighter with 0.17 M DOFs for RANS CFD/CSD based aeroelastic response prediction; Farhat et al. 2003**

For illustration, figures 3 and 4 show state-of-the-art dynamic models of rotary and fixed wing airframes. The details of the work are given later, in the respective survey sections. The emphasis in dynamic models is on the key load bearing components and internal load paths. The emphasis in fluid-structure coupling is on the external shell. For such purposes models which include the outer shell, and in addition, the internal load paths, are most appropriate. For example, Fig. 5, shows a more detailed model of the same F-16, including the outer shell (details of the work is cited later).

Detailed modeling of the fuselage for fluid-structure interaction has not been a key focus so far in rotorcraft for the following reason. The dominant dynamics of a helicopter fuselage, unlike fixed-wing, is vibration, which occurs at high frequencies (usually pN_b/rev). The dominant source of this vibration is not the fuselage flow field, but the shaft transmitted forcing from the rotor. The forcing from the rotor primarily stems from the rotor flow field, the interactional effect of the fuselage on the rotor flow field occurs, nominally, at lower frequencies (1/rev).

There are important conditions where the above argument is invalid. First, at low speed flight (around $\mu = 0.15$) direct impingement of the rotor tip vortices

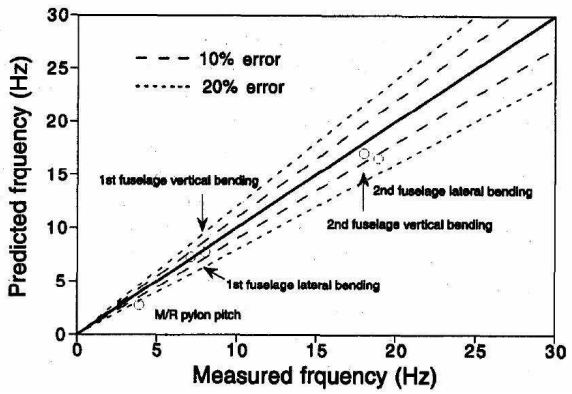

(a) 1-D line fuselage

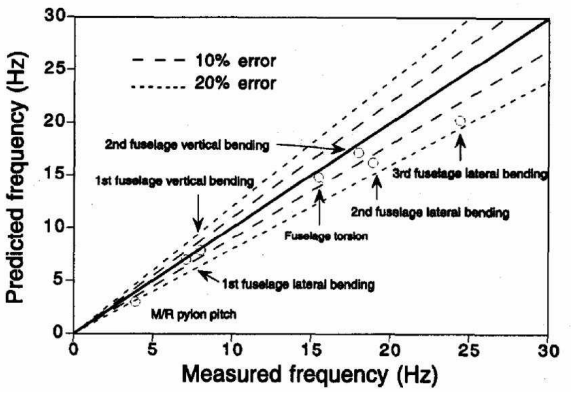

(b) 3-D detailed fuselage

Figure 6: **Measured and NASTRAN calculated fuselage natural frequencies of the AH-1G helicopter; Yeo and Chopra 2002**

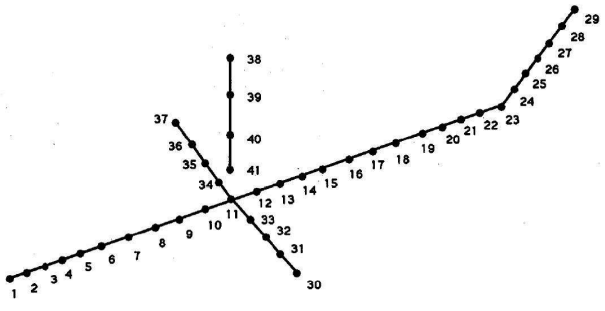

(a) 1-D line fuselage

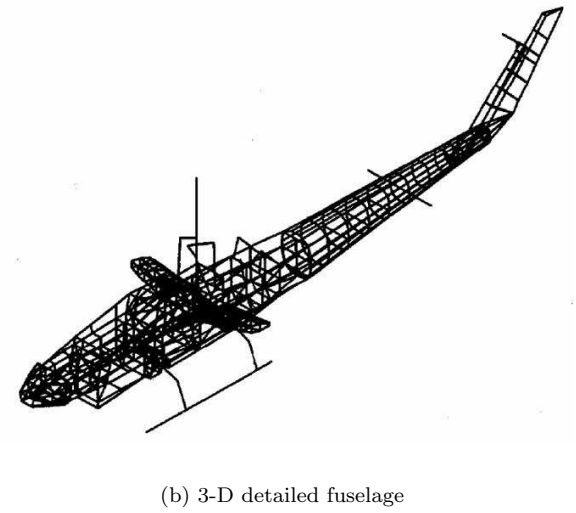

(b) 3-D detailed fuselage

Figure 7: **FEM line and 3-D fuselage NASTRAN models of the AH-1G helicopter from the DAMVIBS program used for rotor-fuselage coupled dynamic analysis; Yeo and Chopra 2002**

on the tail boom is a key mechanism of vibration (at N_b/rev). RANS was unable to resolve this flow field thus far, but is beginning to do so now. Second, for advanced configurations with low shaft clearance (for low drag) direct wake impingement is a significant source of vibration for a wide range of flight speeds. There has been limited resolution of the interactional flow field around the fuselage thus far. RANS based CFD, and alternative wake CFD models like the Vorticity Transport Model [24, 25], are beginning to do so. The emergence of interactional CFD opens opportunity to calculate vibration and buffet loads in response to the interactional flow field.

Reproducing the structural frequencies of the fuselage (need at least up to 30 Hz) is in itself difficult in helicopters (more than 20% error without detail modeling). Difficult components lie in critical load paths (main rotor hub/pylon/transmission case). Dynamicists often use line fuselages to re-produce measured frequencies. For example, the calculated frequencies of an AH-1G (two-bladed, teetering) fuselage for two different types of models are compared with measurements in Fig. 6. The corresponding models are shown in Fig. 7. The simpler model is designed to generate similar frequencies as the more detailed model, and is often preferred. The fluid-structure coupling methodology, however, is more involved for the simpler model compared to the detailed model. The need for extrapolation, a key source of error, is minimized in the case of detailed models that include the external shell structure. Models with both internal and external details of the structure are used regularly by crash researchers, for very short-time high impact transients (less than 0.1 sec). An example of a crash test simulation is shown in Fig. 8, taken from Ref. [26].

Constructing a generalized modular interface which

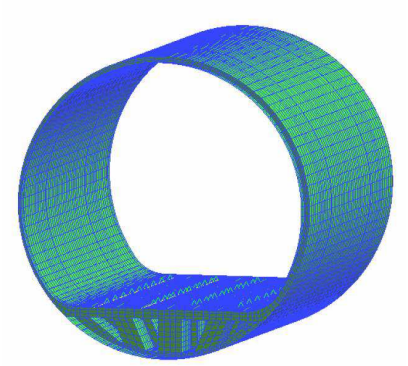

(a) Detailed shell fuselage

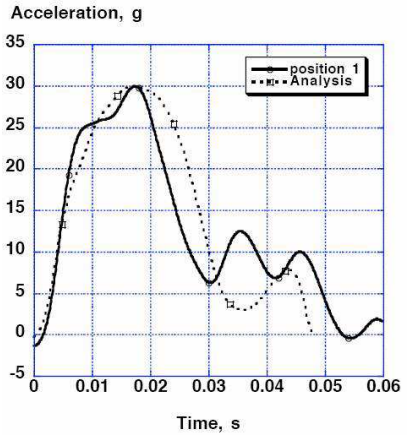

(b) Measured and predicted accelerations at a front left fuselage station

Figure 8: **Detailed FEM composite fuselage (MSC Dytran) as used in high-fidelity crash models; Fasanella et al. 2007 (courtesy Karen Jackson, NASA Langley)**

is adaptable to alternative levels of underlying structural fidelity requires innovative interpolation and extrapolation methods for interface displacement mapping. A large volume of literature has been devoted to such methods for fluid-structure coupling. Broadly, they are divided into two categories. First, the *surface tracking* methods. These rely on the underlying shape functions while trying to mitigate the complexities associated with multi-component sub-structures. Second, the *surface fitting* methods. These are focused more on independent (from fluid and structural solvers) formulations without the need for shape functions. In fixed wing applications, the current practice is to use a combination of these interpolation methods to map deformations from CSD to CFD. Mapping airloads from CFD to CSD then simply amounts to the correct evaluation of virtual work based on the deformation mapping (compare eqn. 8 with eqns. 7 and 12).

A displacement mapping must: (1) recover large deflections and rotations of the underlying structure from the surface displacement, and (2) ensure displacement association with time, i.e. attachment points must remain attached throughout the simulation. Arbitrary procedures like a nearest neighbor mapping, although simple and fast, do not meet these requirements. Moreover, it prevents the correct evaluation of the virtual work term. Procedures which rely on underlying structural shape functions for multi-component blending and extrapolation meet these requirements. They are called surface tracking methods as mentioned earlier. When the shape functions are not available, the most general procedure is to use radial basis functions. These are also called surface fitting methods. The well-known surface fitting methods include the Multiquadric-Biharmonic (MQ) method, the method of surface splines commonly called the Infinite Plate Spline (IPS), the method of Thin Plate Spline (TPS), and Non-Uniform Rational B-Spline (NURBS). These methods have been systematically studied by Hounjet and Meijer [27] in 1994, and Smith et al. [28] in 2000 (see references therein for details of the above methods). The study by Smith et al. found TPS to be most suitable for interpolation and extrapolation of generalized structural geometries. These radial basis functions are defined on the whole domain of a substructure. Complications arise for multiple intersecting sub-structures in 3-D space.

Fitting methods applicable in 3-D, which do not use radial basis functions, have also been implemented, notable among which are the Constant Volume Tetrahedral (CVT) method by Goura et al. [29, 30], and the Inverse Boundary Element (IBE) method by Chen and Jadic [31]. Even though applicable in 3-D, these methods are less suitable for large deformation nonlinear problems. The first method provides a nonlinear mapping. Linearization destroys the exactness of rigid body rotations. The second method requires iterations to conform to the deformed geometry, unless the deformations are assumed to lie within the range of linear elasticity.

An emerging technique is the use of 3-D radial basis functions with compact support. These are defined locally, and hence are easily applicable for surfaces with high 3-D curvature. The method is based on multivariate scattered data interpolation. Originally proposed by Wu [32] and Wendland [33], and subsequently applied by Beckert and Wendland [34] for fluid-structure interaction problems, the method has found increasing application in recent large-scale fixed-wing CFD/CSD calculations [35, 36].

FIXED WING AIRCRAFT

A comprehensive survey of the state-of-the-art in fixed-wing aeroelasticity can be found in Livne [37] in 2003. Schuster et al. [38], in the same year, have reviewed the state-of-the-art in computational aeroelasticity. The term was used broadly, covering unsteady aerodynamics to CFD and beam models to detailed FEM. In 2004, Kamakoti and Shyy [39] described the RANS/FEM coupling procedures used for fixed wing applications. The AGARD 445.6 wing as taken as the baseline configuration for illustration. More recent developments in computational aeroelasticity are highlighted by Bartels and Sayma [40] in 2007. In the same year, a report detailing European research towards the development, evaluation, and transition of high-fidelity aeroelastic tools for full aircraft has also been published [41].

The following sections review the status of computational aeroelasticity in fixed wing applications. The first section briefly describes the status of detailed CSD. The second section summarizes the important aeroelastic phenomena and the status of high-fidelity CFD/CSD methods in predicting them.

Structural Modeling

First, the meaning of 'detailed structures' must be clarified. Shown in Fig. 9 is a typical Boeing 737 wing section with a simple main/aft double flap system with a single slotted thrust gate, in its retracted position [42]. Only the trailing-edge is shown, the three position Kruger slats in the leading edge are not shown. Typical structures such as this, incorporate kinematic constraints to rigid body modes to flexible deformations. For aeroelastic and aeroservoelastic studies, a distinction is made between global and local behavior of structures. Only the global model is coupled to the external flow. The loads generated by the global model are then transferred to the internal structures wherever needed, locally.

The local models handle details, which include FEM of individual composite ply-layups, rigid body mechanisms, redundant load paths, local buckling, crack propagation, stress concentration due to manufacturing imperfections, embedded cooling, and integrated smart materials and actuators. Local effects (e.g. actuator loads, local buckling, composite tailoring) are included via lower order models. The advent of HPC opens opportunity to couple the important frequencies of local analysis directly to global analysis using detailed modeling. Performed judiciously, based on a fundamental understanding of the key phenomena, it can lead to enormous payoffs in design innovation and cost.

A comprehensive treatise on fixed-wing structural analysis and design, as performed in the Boeing Company can be found in Mohaghegh [43]. The philosophy of fail safe design has led to the well-known practice of discretely stiffened wing and fuselage panels and multiply redundant two and three-piece primary bulkheads in the construction of modern aircraft structures. Today, global analysis can be performed using full aircraft FEM and RANS. The structural model involves large-scale but usually linear FEM models. The global loads are then used for internal stress calculations using detailed FEM of the type shown in Fig. 10. Most often, this step involves a static analysis. Since the 1990s, all primary structures of commercial airplanes like the B777 and A340 are certified using such FEM analysis. A typical example is the wing-body junction which includes the cargo bay and landing gear — a region of complex redundant load paths and structural discontinuities, see Fig. 11. The need for analysing such structures led to the original development of sub-structuring methods. Composites materials are used on selected components like the radomes, fairings, all control surface panels, engine nacelles, and torque boxes. The main purpose is to provide higher impact, fatigue, and corrosion resistance.

Almost every modern rotor blade is an all composite construction (although the main spar is frequently of Titanium construction). The internal layout of rotor

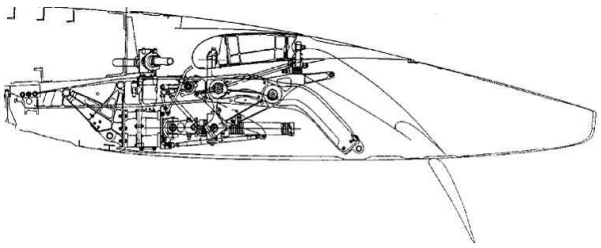

Figure 9: **The outboard wing cross section of a Boeing 737-NG aircraft; van Dam 2002**

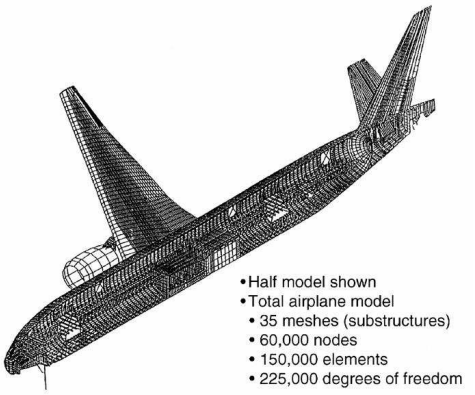

Figure 10: **A Boeing 777 FEM stress model with details of major internal components; Mohaghegh 2005**

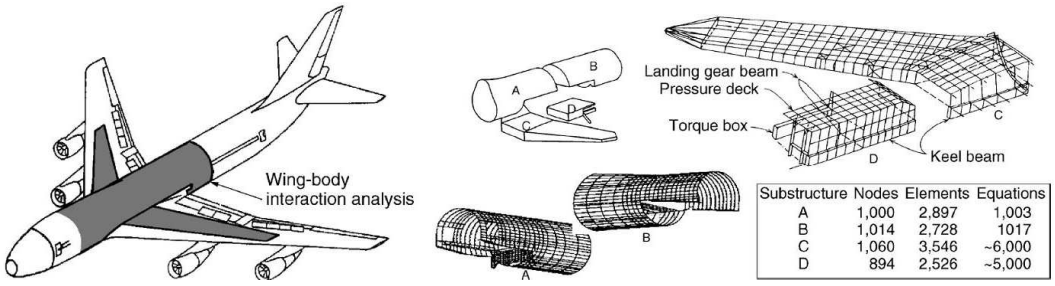

Figure 11: **A routine Boeing 747 wing-body interaction FEM stress analysis model with typical substructures; Mohaghegh 2005**

blades, however, are much simpler compared to the mechanical complexity of fixed wing sections. The control mechanism for conventional main rotors are all essentially concentrated at the root end. In the case of rotors, the state-of-the-art in global and local models are 1D beam FEM and 3D stress analysis respectively. The 1D beam properties are first obtained by a separation of the 3D problem into a 1D problem and a 2D cross-sectional analysis problem (see section on rotary wing). Analogous to its aerodynamic lifting-line counterpart, the theory is not meant for end stresses or stress concentrations at the attachment point. More importantly, the root end flex-beams and torque tube structures of modern hingeless and bearingless rotors require that the external loads be transferred correctly to internal stresses. This is currently performed by a detailed re-calculation using commercial FEM codes like ABAQUS, ANSYS, etc, in a static fashion (using the dynamic forcing obtained from the global model). It is desirable that future HPC based simulations make this approximate re-calculation redundant.

While the 1-D beam FEM model of a rotor blade is comparatively simpler, the models include geometric nonlinearities rigorously that are critical for rotors. Rotary wing aeroelasticity is inherently nonlinear, the nonlinearities stem from the centrifugal and Coriolis forces due to blade rotation. The Coriolis nonlinearity is in turn coupled with the rotor trim state. This level of coupling between CSD and vehicle dynamics is absent in fixed wings, and this has its implications on the efficiency of methods that couple rotorcraft CSD with CFD.

Aeroelastic Phenomena and CFD/CSD Predictions

Flutter

Flutter analysis in subsonic regimes are satisfactorily performed by standard k and $p-k$ methods using doublet-lattice type linear aerodynamic models. These options are available today as part of FEM codes like NASTRAN and ASTROS. In supersonic regimes, methods related to piston theory are used. A description of the current status of these methods, along with their aeroelastic applications, can be found in Yurkovich [44]. High-performance fighter aircrafts are, however, flutter critical in the transonic regime where unsteady shock motions of three different types determine the nature of energy transfer between the fluid and the structure. A linear structure is still enough, only the aerodynamic nonlinearities need to be predicted. Hence high-fidelity RANS CFD approaches are sought.

Unlike helicopter blades, where flap-lag flutter of hingeless rotors is determined by structural nonlinearities coupled to the vehicle operating state, fixed wing bending-torsion flutter is a linear phenomena. The effect of vehicle g-level is only via the effect of trim angle of attack on the shock motion. At a given angle of attack, and dynamic pressure, a conceptually straight-forward fluid-structure transient response can be used to extract the frequency and damping. Because classical logarithmic decay methods are sensitive to noise, refined eigensystem realization algorithms are used to extract these parameters for the particular modes of interest. Most often (except for free-body control surface flutter) these are the first few antisymmetric modes of the aircraft. Depending on the convergence and divergence of response, generally 5 to 6 transient calculations are enough to bracket a flutter point (i.e. a frequency, damping vs. dynamic pressure point corresponding to zero damping at a given Mach number).

One of the early CFD based flutter calculation for a complete aircraft was performed by Melville in 2001 and 2002 using Euler [45] and RANS [46] coupling, for a F-16 fighter aircraft. The linear FEM structural model used was the same as used by Denegri earlier [47] for a doublet-lattice based flutter analysis. Ten symmetric and ten anti-symmetric mode shapes were considered. An extra mode was incorporated for the leading edge flap. The flap was represented as a damped first-order system that relaxed into a commanded position. The FEM model is shown in Fig. 12(a). It was built from several simpler models representing each of the main components

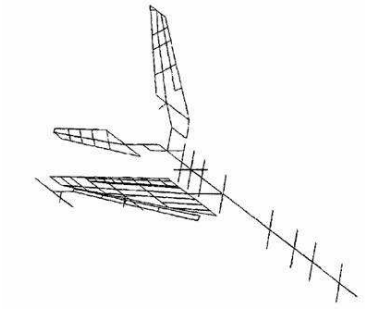

(a) FEM structural model

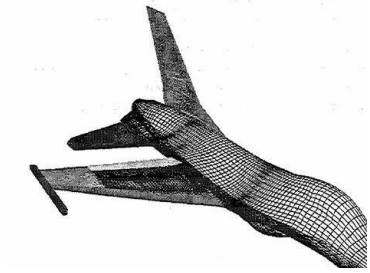

(b) Fluid-structure interface geometry representation

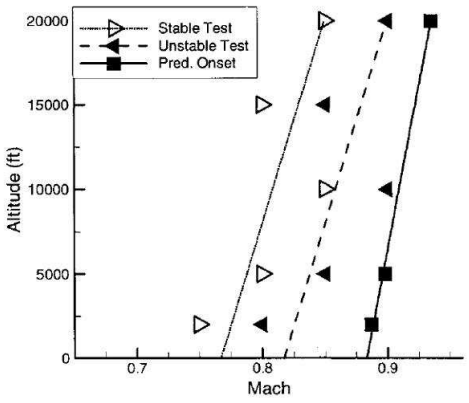

(c) Measured and predicted flutter boundary

Figure 12: **Measured and predicted flutter onset boundaries for a F-16 fighter aircraft using RANS/FEM modal coupling; Angle of attack α=1.5°; Melville 2001, 2002**

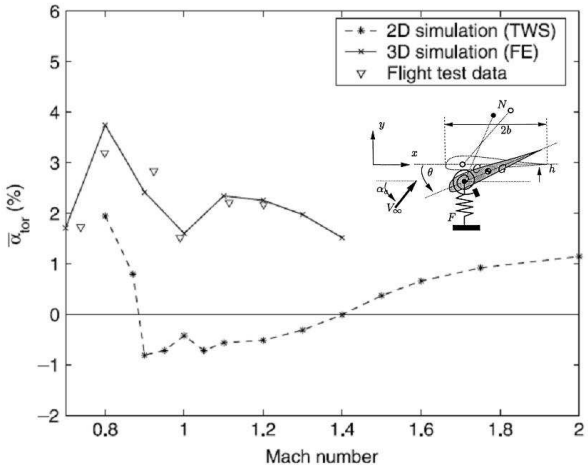

(a) Predicted and measured torsion mode damping

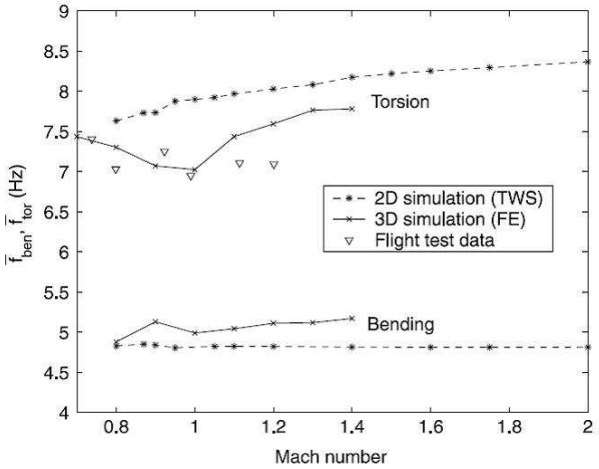

(b) Predicted and measured bending / torsion frequencies

Figure 13: **Predicted and measured aeroelastic parameters for a F-16 fighter aircraft at 3000 m altitude using RANS/full FEM coupling; Farhat et al. 2003**

— the fuselage, wings, leading-edge flap, flaperon, tip launcher, and tails. The fluid-structure interface representation was constructed by seperate extrapolation of each component. The interface is shown in Fig. 12(b). The curvature was provided by the underlying structural components, extrapolation to surface was done linearly. The RANS domain (Baldwin-Lomax) contained 20 to 36 overset grids with 1.9M to 3.5M points. The details of the inlet, exhaust, ventral fins and under-wing store were not included. The coupling method and the moving grid mechanism (with its associated Geometric Conservation Law) was based on an earlier work by Morton et al. [48]. A single CPU was used for structures and grid deformation, the fluids solver was run in parallel.

A perturbation response damped the three primary symmetric modes into steady deflections. The three primary anti-symmetric modes were lowly damped and showed zero mean oscillations. The conventional procedure for extracting modal damping is to use classical logarithmic decay methods. For a full FEM model, real-time parameter identification methods, as used in flight tests, are used. The procedure is recognized as a challenge in

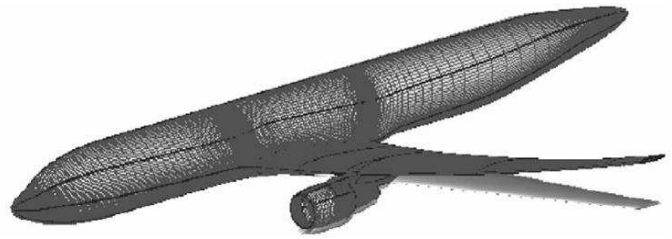

(a) A Boeing twin-engine transport wind-tunnel model

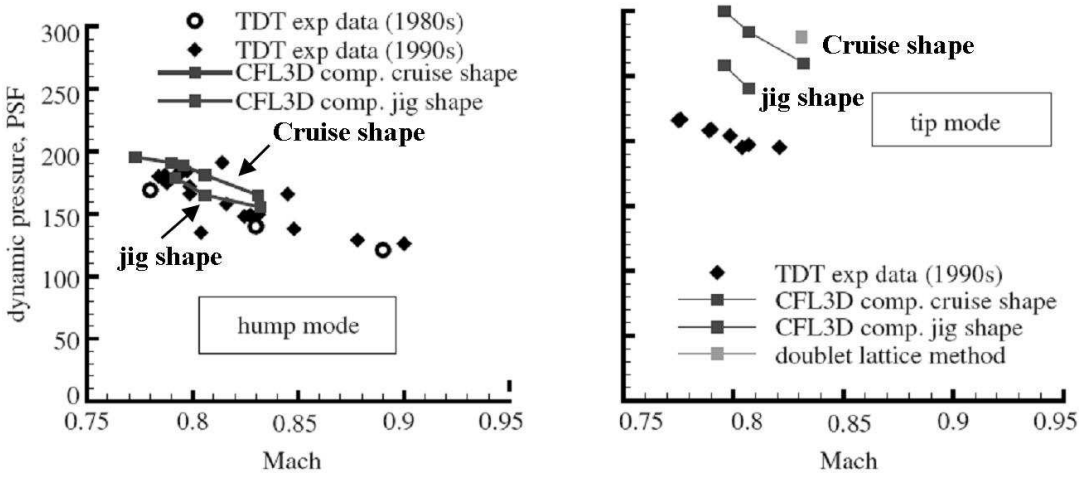

(b) Transonic flutter onset dynamic pressures for a hump mode and a tip mode

Figure 14: **Predicted and measured flutter onset for a twin-engine Boeing transport aircraft model using RANS/FEM modal coupling; Hong et al. 2003, reproduced from Bartels and Sayma 2007**

general. Often, a doublet-lattice based linear analysis is performed a priori to identify the critical modes. In this particular instance for example, linear analysis results from Denegri [47] was used to identify the second mode as the critical mode. This mode was then tracked during the CFD/CSD simulation. Figure 12(c) compares the predicted flutter boundary with flight test data.

Farhat and his co-researchers [49, 50] have performed RANS/full FEM simulations of the same aircraft. The structural model was that shown earlier in Fig. 5. It contained around 0.17M linear DOFs comprised of bar, beam, solid, plate, shell, and composite elements. The fluid solver was run on up to 24 CPUs on an SGI Origin 3200 computer with parallel speed up of 21. Of the total CPU time, 60% was spent on fluids, 38% in mesh deformation, and only 2% on structures. The authors note that for nonlinear (geometric) FEM, the structures require 15% of time. The total time for one transient calculation on 24 CPUs was 2.5 hours. An Eigensystem Realization algorithm was used to extract the frequencies and damping of the two lowest modes, see Fig. 13. The algorithm requires only two cycles of history as long as the sampling rate is 500-1000 Hz. A typical wing-section analysis using 2-D CFD coupled to a 2-DOF spring-mass system was also performed for comparison. Recently in 2007, Lieu and Farhat [51] have used the same test case to systematically compare these results with those obtained using Proper Orthogonal Decomposition based reduced order aerodynamic models.

A description of the status of RANS based flutter predictions in commercial aircraft design can be found in the review paper by Bartels and Sayma [40]. A collaborative Boeing-NASA effort recently examined flutter onset on a half-span twin-engine transport model including the aerodynamic interactions of the wing, nacelle, and strut, the effect of wind tunnel wall, and the effect of static aero. The details of the work originally appeared in Hong et al [52], and are reproduced here in Fig. 14 from reference [40]. The CFD code used was CFL3D (version 6), which coupled RANS to structural modes. A second-

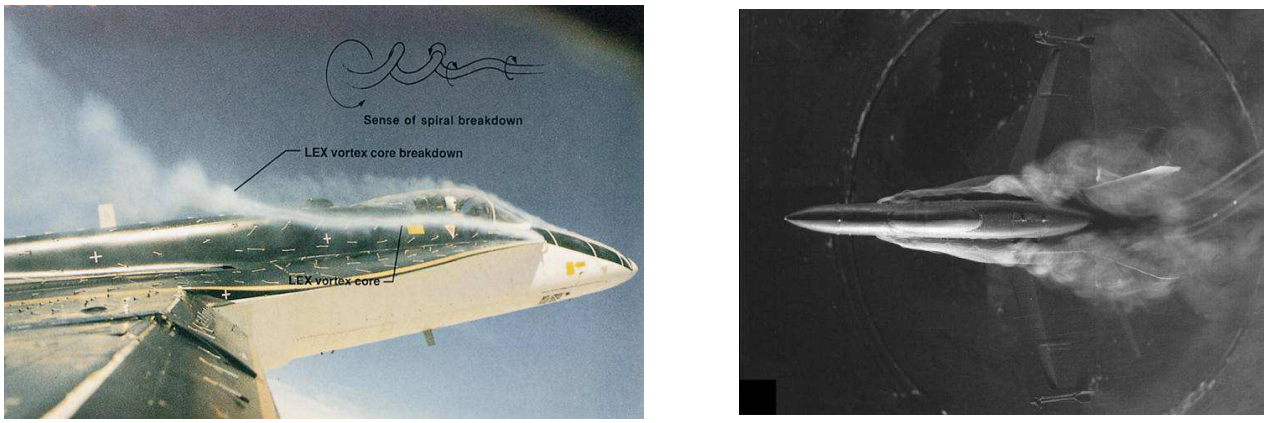

(a) Flight test

(b) 1/72-scale model test

Figure 15: **Flow visualization of LEX vortices; (a) An LEX vortex on a F/A-18 High Angle-of-attack Research Vehicle (HARV), wing-tip view at α=25°, β=-1.4°; (b) A 1/72-scale model plan view at α=30°; Lee 2000**

order predictor-corrector based coupling was used in this study between the fluid and structure. The model exhibited a 'hump' mode, i.e. a lightly damped mode which is unstable only on a limited range of dynamic pressure. The analysis predicted this mode. Predictions for another unstable mode, the tip mode, showed inconsistent results. Predictions showed greater error when the actual cruise shape was used compared to the undeformed jig shape.

Tail Buffet

Fixed-wing tail buffet studies date back to the 1930s and officially began with a Junkers F13 ge monoplane crash in Meopham in England. The official British investigation attributed the tragic accident to horizontal tail buffeting. Subsequently, early work focused mostly on horizontal tail buffet. Since the late 1970s and 80s the buffet problem has received renewed attention with the introduction of the F-14, F-15, F-16 and F/A-18 fighters in the US Air Force and Navy. This time, the focus has been on vertical tail buffet.

Modern fighters are designed with maneuver capabilities at high angle of attack (AOA), typically 25° to 35°, sometimes as high as 60°. To generate lift at these high AOA, a Leading edge EXtension (LEX) is designed on each wing to create two vortices that trail downstream over the aircraft. At the same time small disturbances from the fore-body are also reinforced by the two LEX vortices. The vertical tails (also called fins) which provide directional stability and control, are placed to take full advantage of these two vortices. However, if the vortices fail to traverse the adverse pressure gradient on the wing, and burst, they impinge on the tail instead and produce large vibration and consequent fatigue damage. This phenomena is called tail buffet. Figure 15 shows flow visualization of vortical flows that produce tail buffet.

Tail buffet without the interaction with LEX vortex have also been reported. For example, on the F-15, the main wing vortex system generated buffet loads. It is only for the F/A-18 aircraft that a large volume of experimental and analytical studies exist for a systematic understanding of the problem. Lee [54] in 2000 has comprehensively described the problem, and reviewed the status of fundamental understanding, experimental data, and analytical predictions of the tail buffet. The problem has acquired increased relevance as the three largest U.S. fighter aircraft programs have twin tails, F/A-18E/F, F-22, and the F-35 (Joint Strike Fighter).

There have been several noteworthy attempts at alleviating tail buffet from the late 80s through 90s using extensive wind tunnel and flight tests. The only method used today is the LEX fence developed by McDonnell Douglas Corporation via trial and error using wind tunnel experiments and flight tests. The LEX fence is a flat trapezoidal plate standing on the LEX upper surface aligned in a stream-wise direction.

The complexity of the problem and its sensitivity to flight conditions and aircraft configurations makes it ideally suited for a high-fidelity analysis. At the time of Lee's review there was only limited RANS calculation of the tail buffet problem. These early calculations were by Rizk and Gee [55] in 1992, Ghaffari et al [56] in 1993, and

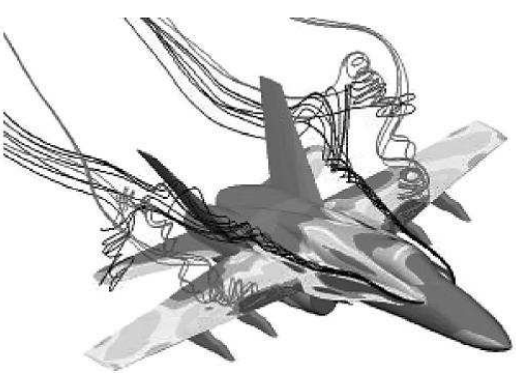

(a) Instantaneous streamlines of LEX and wing vortices without LEX fence

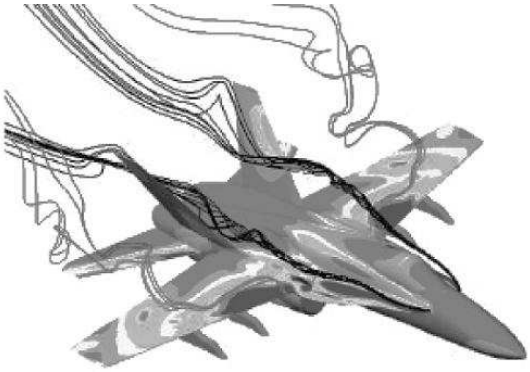

(b) Instantaneous streamlines of LEX and wing vortices with LEX fence

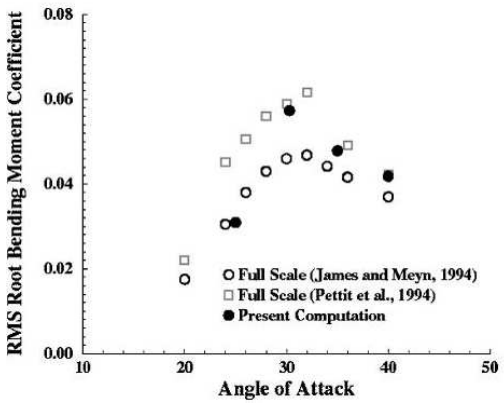

(c) Without LEX fence

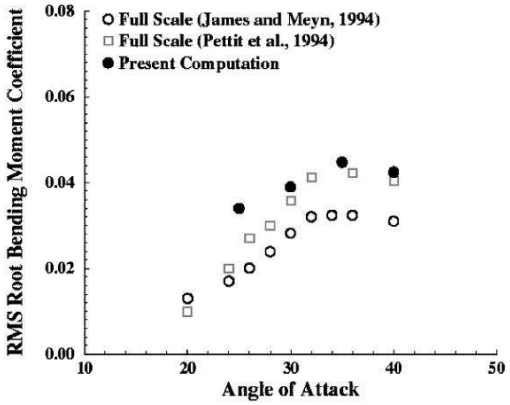

(d) With LEX fence

Figure 16: **Predicted and measured tail bending moments during F/A-18 tail buffet alleviation using LEX fences; RANS/FEM coupling, FEM of vertical tail only; Bending moments are integrated differential pressure moments, not structural gauge loads; Sheta 2004**

Gee et al. [57] in 1996. These studies focussed on CFD, the structure was assumed to be rigid, and had limited success in predicting structural buffet loads on the tail.

A RANS/FEM prediction of buffet loads on the F/A-18 tail was carried out by Sheta in 2004 [58]. The study clarified the fundamental contribution of the LEX fence in alleviating buffet loads. The aircraft was assumed to be rigid, but the tail was modeled using 3-D hexahedral brick FEM (isotropic, Aluminum). The RANS domain had 53 structured blocks with a total of 2.68 M grid points. The total time required on 6 CPUs (of 1.0 GHz speed each) was 142 h. Figure 16 shows the predicted flowfields and tail bending moments from this study with and without the LEX fences. The off-body flow was considered to be laminar in this study.

Recently, Morton et al. [59] have used detached-eddy simulation (DES) based turbulence model for a more meaningful calculation of vortex breakdown. DES is a popular RANS/LES hybrid model. It uses RANS in the boundary layer and LES in the regions of massive separation. Designed primarily for external flows, it can be implemented by a relatively simple modification of an existing Spalart-Allmaras (S-A) RANS model in an unsteady solver. The LES domain does not require an explicitly defined SGS model. The modification to the S-A model automatically implies the existence of a Smagorinsky-type SGS model under the assumption of local equilibrium between the production and dissipation of eddy viscosity. The simulations were performed for the F-18 High Angle-of-Attack Research Vehicle (HARV). For the chosen flight condition, the F-18 HARV configuration matches an F/A-18C configuration with leading-

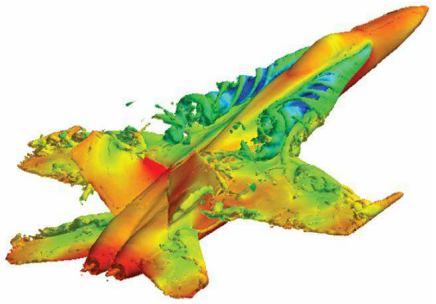

(a) LEX vortex breakdown around a F/A-18 aircraft using DES model

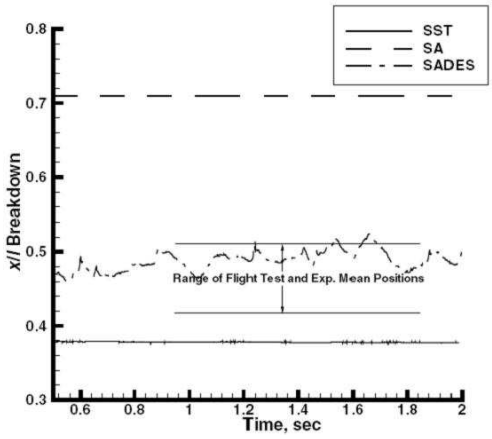

(b) Vortex breakdown location (nose is x=0) validated with flight test data

Figure 17: **RANS calculation of vortex bursting and tail impingement using Detached Eddy Simulation (DES); no LEX fences; Morton et al. 2007**

edge flaps set to -33°, trailing-edge flaps set to 0°, and the diverter slot through the LEX fence closed. The angle of attack was 30°, Mach number 0.2755, Reynolds number 13M (corresponds to altitude of 20,000 ft). The DES simulations were performed on a baseline unstructured grid of 3.6M cells (using the commercial CFD code Cobalt). A time-averaged solution was used to produce an AMR grid with 3.9M cells using Pirzadeh's grid adaptation method [60]. The analysis, however, did not include a structural dynamic model; the focus was on the flow field.

Limit Cycle Oscillations (LCO)

Fundamental understanding of LCO and its satisfactory prediction remain beyond the state of the art in fixed-wing aeroelasticity. The LCO is a general term. In fixed wing fighters it is characterized by sustained, periodic, antisymmetric oscillations of the wing which are not catastrophically divergent. Inside the fuselage, it is felt as a lateral motion. It has been a persistent problem since the mid-1970s in high subsonic and transonic speeds for configurations with missiles on the wingtips and heavy stores on the outboard pylons. The F-16 and F/A-18 fighters with wing tip missile launchers traditionally encountered LCO. Similar phenomena are expected for the F-22 and F-35 as flight tests begin.

Bunton and Denegri [61] presents an insightful commentary on fixed-wing LCO. The phenomenon is similar to classical flutter, in that the oscillations occur at a single frequency close to that predicted by linear flutter. The mode shape, at the onset, also resembles that predicted by linear flutter. In level flight, the onset speed lie quite close to that predicted by linear flutter. As a result LCO has been termed limit cycle flutter or constant amplitude flutter by many, a terminology not preferred by others as the word 'flutter' has historically referred to catastrophic divergence. Many speculate that the genesis of LCO is not the classical bending-torsion flutter at all, but the aircraft flight control system.

During LCO, the amplitude remains constant for a given, stable flight condition. If the aircraft is accelerated to a higher speed, the amplitude would increase and settle into a higher level once the higher speed is reached. If an attempt is made to back out of LCO, the oscillations often persist below the original onset values (hysteresis). In addition to LCOs involving the entire aircraft-wing store structure, LCOs can occur involving localized nonlinearities like control surface free-play.

LCO occurs both in level flight as well as in high load factor maneuvers. Usually the onset speed is lower in the latter. Compared to LCO onset in level flight, those occurring in maneuvers are much less predictable. For example, LCO magnitudes can increase from 1g to 4g and then begin decreasing so as to disappear at 5.5g [61]. For a different store configuration there may not be any LCO at all until 5g, at which LCO begins, and grow so rapidly so as to resemble the onset of classical catastrophic flutter. The key unresolved challenge, beyond that of predicting the onset, is predicting the magnitude of LCO. In fixed wing, unlike rotorcraft, the fatigue of components is of lesser concern compared to the limit loads. (Fatigue concerns are evident however for test aircraft repeatedly exposed to flutter tests and LCO.) LCO concerns are related to weapons accuracy for smart and unguided weapons, and reliability of ordnance release. The transonic aerodynamic nonlinearity that can lead to LCO has been explained by Bendiksen [62] based on the categorization of shock motions by Tijdeman and Seebass in 1980 [63]. It was shown that, for a clean wing, when a bending-torsion flutter mode triggers a transition from

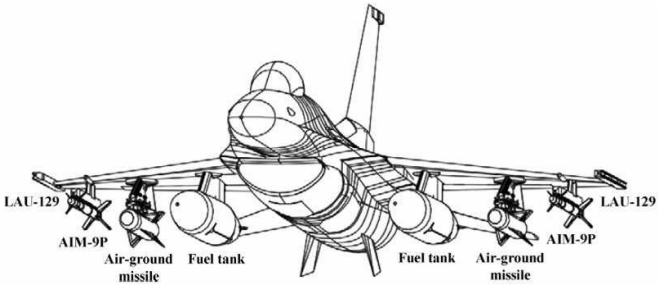

(a) External stores on a F-16 fighter during flutter and LCO flight tests

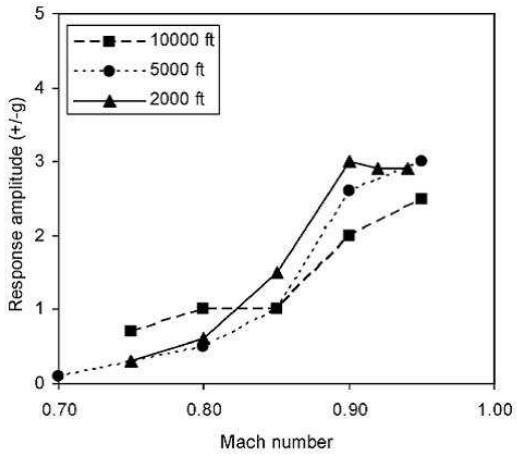

(b) Measured maximum wing-tip LCO response in level flight

Figure 18: **Measured wing-tip LCO deformations of a F-16 fighter aircraft with under-wing stores; Denegri et al. 2005**

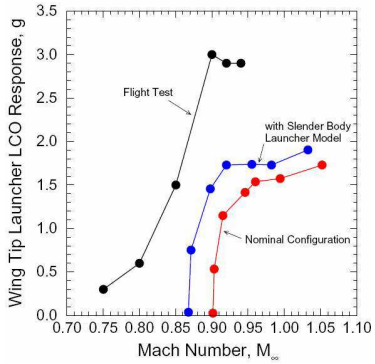

(a) Configuration 1

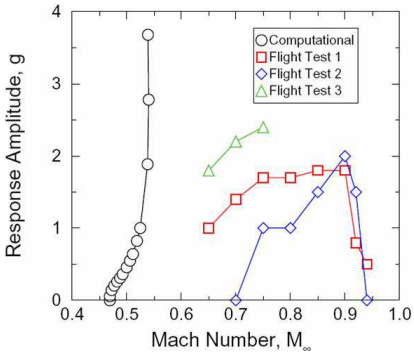

(b) Configuration 2

Figure 19: **Predicted and measured LCO magnitudes using RANS CFD/FEM coupling in level flight; (a) Effect of slendor body-wing model for launchers, (b) LCO predicted only with launcher model; Thomas et al. 2007**

type-A (shock motion oscillates sinusoidally) to type-B (shock disappears during a downstream motion) shock motion, then the associated rapid decrease of aerodynamic work done per cycle can lead to LCO. The role played by under-wing stores and structural nonlinearities including free-play are more configuration specific. As flight testing becomes more and more expensive, and the number and combinations of under-wing store configurations increase, higher-fidelity methods are ideally suited for a comprehensive attack on the LCO problem.

One of the early high-fidelity attempt to simulate LCO was that of Melville in 2002 [46] described earlier in the section on flutter. While calculating the onset of flutter he investigated whether the undamped response (or lowly damped response near the flutter boundary) resembled an LCO as seen in flight. What distinguishes an LCO response from a zero-damping periodic flutter point is that the LCO amplitude is independent of the initial excitation, and depends only on the underlying limiting mechanism. The second mode excitation, when calculated with different set of initial excitation, settled to a different amplitude (proportional to the initial excitation). Thus it was not LCO.

More recently, in 2005, Denegri et al. [64] have generated benchmark LCO data for the F-16 aircraft. A sample of benchmark measured LCO deflections along with the associated wing measurement locations are shown in Fig. 18. Oscillation frequencies range from 7.9Hz to 8.2 Hz with lower frequencies around Mach 0.9.

In 2007, Thomas et al. [65] have used a nonlinear harmonic balance based RANS solver to calculate the LCO magnitudes for different configurations of the F-16. A slender-body wing-theory was used to model the ex-

ternal weapons and wing stores and study their impact on LCO prediction for eight different weapons and store configurations. A comparison of the predicted LCO magnitudes with those of measured data, as in Fig. 18(b), is given in Fig. 19(a). It corresponds to 2000 ft altitude, 1.5° angle of attack flight test. The figure is sufficient to highlight the poor state of affairs in LCO prediction. Figure 19(b) compares predictions for a different configuration, but at the same altitude and angle of attack. The LCO could at least be predicted with the wing store model.

Parker et al. [66] have carried out systematic studies on the effect of under-wing stores on LCO using a simple rectangular cantilevered wing model. The details of the wing model can be found in [67]. The model is based on Eastep and Olsen's heavy version [68] of the original Goland wing [69]. They found that the role of store aerodynamics was to transfer additional energy into the structure increasing the magnitude of limit cycle oscillation.

In addition to the F-16 and F/A-18, LCO studies have been documented on a B-1 like configuration [71] and on a B-2 bomber. The latter phenomena is now well-known as the Residual Pitch Oscillation (RPO) and has been studied by Dreim and his co-researchers [72] using the Computational Aeroelasticity Program - Transonic Small Disturbance (CAP-TSDv) code.

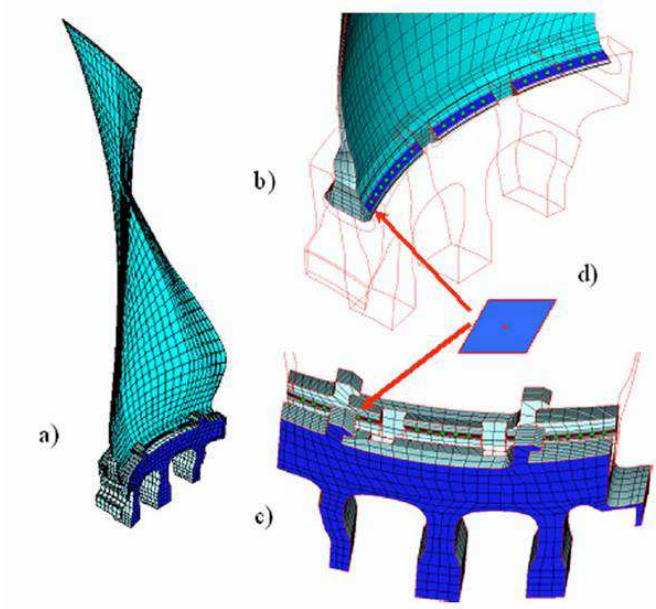

Figure 20: **FEM model of bladed disks: (a) a disk sector; (b) blade contact surface; (c) disk contact surface; and (d) an area contact element; Petrov and Ewins 2006.**

TURBOMACHINES

The advances in fundamental understanding, analysis, and prediction of turbomachinery aeroelasticity can be broadly traced from 1970s to the present time by survey papers in Mikolajczak et al. in 1975 [73], Bendikson in 1990 [74], Marshall and Imregun in 1996 [75], and Bartels and Sayma in 2007 [40]. The historical evolution of the aerodynamic methods has been traced recently by Cumpsty and Greitzer [76]. Structural dynamics (and flutter) has been surveyed by Srinivasan in 1997 [77], Slater in 1999 [78], and more recently Castanier and Pierre in 2006 [79].

The purpose of the following sections is to review the status of turbomachinery high-fidelity computational aeroelasticity. As in the case of fixed wing, the focus here is again on CSD, and coupled high-fidelity CFD/CSD methods. The first section summarizes the status of detailed CSD. The second section summarizes the key aeroelastic phenomena, and the status of CFD/CSD in predicting them.

Structural Modeling

Finite element models of turbine blades comprise of millions of DOFs made up to 3-D linear solid elements. Commercial FEM packages like ANSYS and ABAQUS are routinely used for industrial as well as research purposes. Turbine blades are made out of nickel based single-crystal super alloys. In addition to unsteady stresses, turbine blades have to endure high temperature (particularly during start-up and shutdown) and exposure to high-pressure hydrogen (in case of internal coolant). Furthermore, the blades are prone to severe fretting by the root end friction damper, and contact damage at the dovetail attachments which can lead to crystallographic initiation and crack growth. Detailed 3D FEM analyses are carried out with special surface-to-surface contact elements for such purposes, see for example Arakere et al. [80] and the references therein.

The forced response of bladed disks are affected by contact surfaces at the blade-disk dovetail attachments, part-span interlocking shrouds, and under-platform friction dampers at the root. These components are used to avoid dangerous resonance regimes. Significant amount of research is conducted to model these discontinuity phenomena within 3-D FEM. Recent work on 3-D FEM modeling of dovetail attachments can be found in Beisheim and Sinclair [81]. Recent work on modeling of under-platform friction dampers can be found in Petrov et al. [82, 83]. Figure 20, taken from the latter work, illustrates the placement of an area contact element within a typical FEM model of a bladed disk.

When all sectors of a bladed disk are similar, the

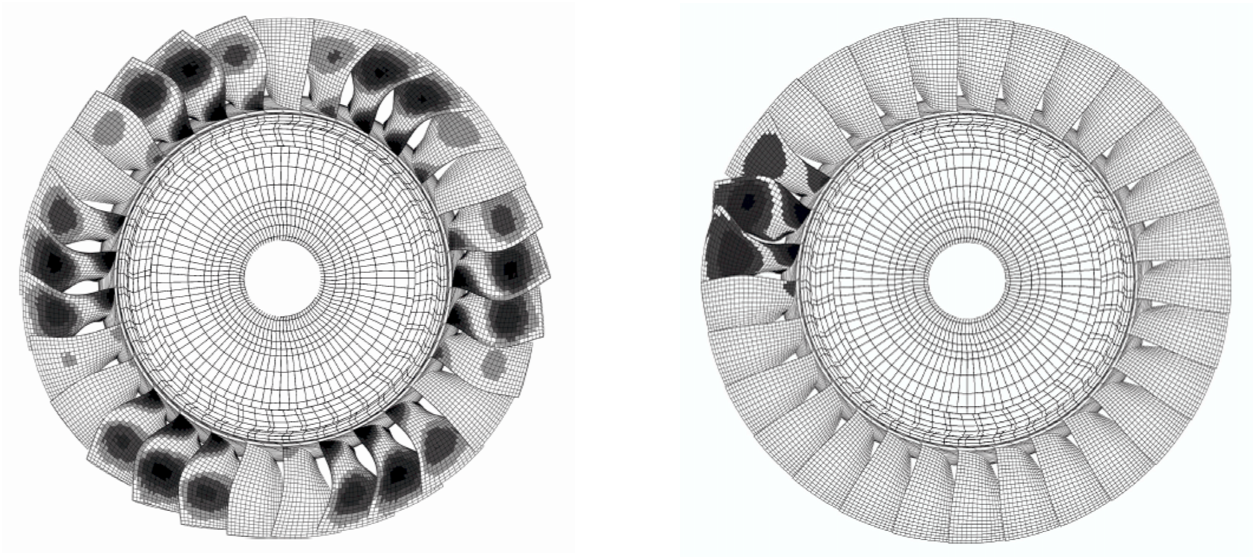

(a) Three nodal diameter mode of a tuned bladed disk

(b) Localized mode shape of a mistuned bladed disk

Figure 21: **Mode shapes of a tuned and mistuned modern bladed disk; Castanier and Pierre 2006**

structure is called tuned, or having cyclic symmetry. The analysis can then be simplified to one or a few sections. Mistuning destroys cyclic symmetry and produces mode localization in a bladed disk. This phenomena is particularly important for High Cycle Fatigue (HCF), where high localized stresses can lead to failure. Figure 21 shows an example of a modern bladed disk FEM model showing the effect of mistuning on mode shapes. Studies on mistuning have received attention since 1970s, led by the pioneering work of Whitehead [84] and Ewins [85]. However, it is only recently that the emergence of whole annulus multi-row CFD have made reliable forced response predictions of mistuned bladed disks appear feasible in near future. For a recent review of the various modeling and analysis techniques, and the assessment of mistuning sensitivity, see Ref. [79]. The mode localization due to mistuning, as mentioned earlier, is more pronounced in the presence of frequency veering. Frequency veering is a common phenomenon in rotating structures. Coupled modes approach each other with increase in RPM and veer away after exchanging mode shapes due to changing contributions of centrifugal loading in each. The same phenomena occurs in helicopter blades, except that the low aspect ratio of the turbine blades (around 1.5–3 compared to 10–15 for rotorcraft) and the large flexible disk compress a larger number of vibration modes within a smaller frequency range which are richer in interaction. A unique phenomena, not to be found in rotorcraft blades, is the interaction between disk dominated and blade dominated modes. It is observed, that the sensitivity of a bladed disk to mistuning increases with frequency veering. Recent work on mistuning and mode localization can be found in Petrov and Ewins [86], Rivas-Guerra and Mignolet [87], and Kenyon et al. [88, 89].

The whole annulus treatment of a bladed disk, with or without mistuning, is in itself an idealization which holds true only for isolated, dynamically independent rotors. A disk with identical blades is not necessarily tuned, particularly for multi-stage compressor blades. The modes of one stage interact with those of its neighbor, which usually contains a different number of blades giving rise to mistuning of the coupled stages. Unlike helicopters (co-axial) the stage to stage spacing is only a fraction of the blade chord. In addition, the disk is large and flexible, compared to the hub in helicopters. Bladh et al. [90] have studied the effects of structural coupling of multi-staged bladed disks, see Fig. 22.

Aeroelastic Phenomena and CFD/CSD Predictions

Aeroelastic Phenomena

A modern turbofan engine and a schematic illustrating its instability prone components are shown in Fig. 23.

Static aeroelasticity in turbomachines deals with the calculation of blade un-twist and un-camber because of high centrifugal and pressure loads. There is no divergence phenomenon. Typical un-twists can be around 5° and changes the stagger angle. The manufactured shape

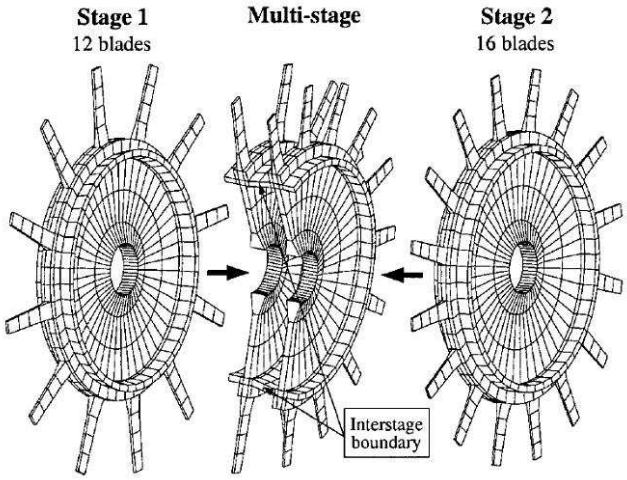

(a) FEM for single and two-stage rotor models

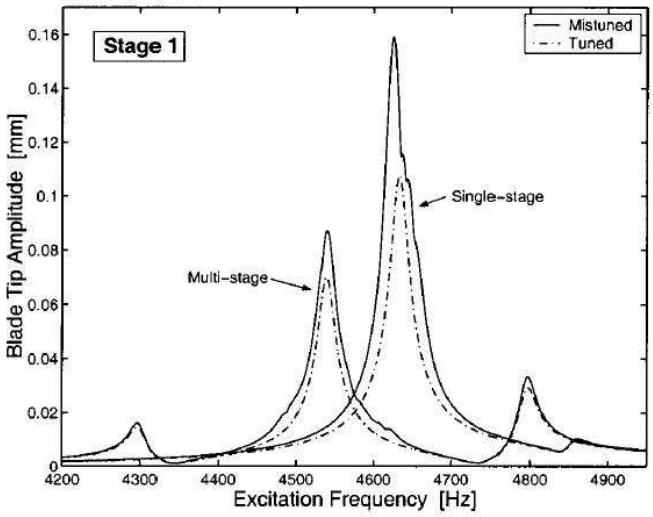

(b) Stage 1 forced response from Engine Order 10 excitation, using tuned and mistuned FEM single and two-stage models

Figure 22: **Effect of multistage rotor structural coupling in turbomachines; Bladh et al. 2003**

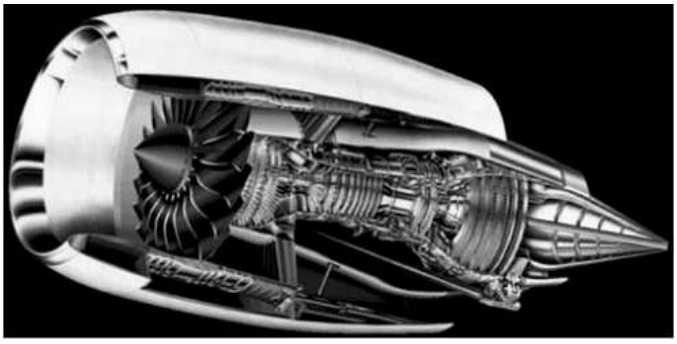

(a) The GE 90-115 B growth engine of the Boeing 777

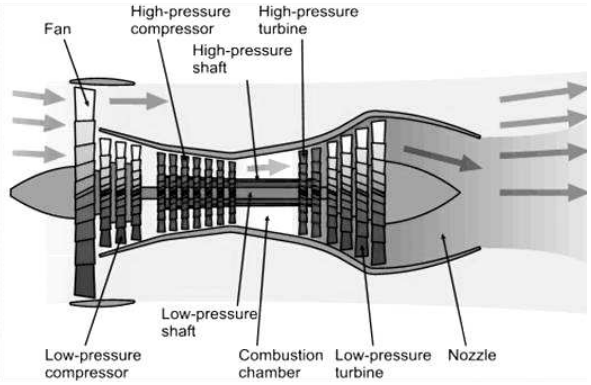

(b) Schematic of a modern turbofan

Figure 23: **The components of a modern, high bypass ratio turbofan engine**

(cold) is calculated based on the anticipated un-twist and un-camber of the operating shape (running). The effect is pre-dominant in fan blades. A recent study can be found in Wilson et al. [91].

Forced response is most critical for turbine blades. The High Cycle Fatigue phenomenon is a major issue is gas turbine blades. In addition to unsteady forcing, high thermal stresses and internal coolant pressure lead to fatigue failure. The U.S. Air Force estimates that 55% of jet engine safety Class A mishaps (over $1 million in damage or loss of aircraft) and 30% of all jet engine maintenance costs are due to HCF [92]. The forced response phenomenon also occurs in compressor blades. But here, it occurs not only at Engine Order (EO) excitations (similar to blade passage frequency in helicopter main rotors), but also at Low Engine Order excitations (LEO). The latter arise due to stage-to-stage interactions. Compared to turbines, compressors typically have greater number of blade stages which produce a greater number of engine order excitation frequencies.

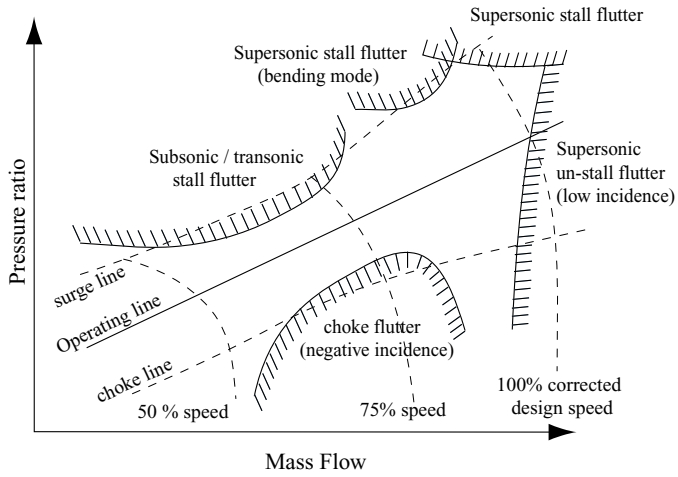

Figure 24: **A typical compressor map showing the various flutter boundaries**

Flutter occurs in fan blades, the front stages of axial compressor blades, and occasionally in the low pressure turbine blades. Fan blades are the most flexible components, especially those in the high bypass ratio commercial airplane turbofan engines. In case of compressors, demands of increasing pressure ratios and weight reduction result in highly loaded stages operating in transonic inflow. In addition, the front stages are subjected to severe inlet flow distortions.

The nature of flutter is complex in turbomachines, and the fundamental mechanisms are often difficult to distinguish. Conventionally, the various flutter regions of a compressor are demarcated as shown in Fig. 24. The mass flow is a corrected value, i.e. an equivalent mass flow under ambient conditions. The pressure ratio is the ratio of exit stagnation pressure to inlet stagnation pressure of the compressor. The surge line is the highest operating line above which the airflow can reverse abruptly creating rotating stall, called surge. The subsonic and supersonic stall flutter are two of the more distinct regimes. The subsonic stall flutter occurs in part-speed conditions when the inlet flow is high subsonic or transonic. Typically, they are a Single Degree of Freedom (SDOF) torsion mode flutter. The supersonic stall flutter occurs at high-speed operating conditions when the inlet flow is supersonic and contains detached leading edge shocks. Often, they are a SDOF bending mode flutter. A SDOF flutter, unlike a classical frequency coalescence type bending-torsion flutter involves energy exchange between a single mode and the fluid. The driving phenomena in compressors are either oscillating shock waves or stalled flow. A simple linear structural model is enough as long as the aerodynamic damping is correctly evaluated. The complexity mainly lies in the latter task.

CFD/CSD Predictions

The 1990s saw the development of large scale parallel solvers for unsteady aerodynamics in turbomachines, see for example Refs. [93, 94, 95]. The high computational requirements restricted the simulations to a single stage. More recently, solvers with massive parallelism, i.e. with demonstrated scalability on 100s of CPUs have been developed [96, 97]. For example, the Stanford University code TFLO2000 has been tested for scalability on 1024 processors for a model problem with 9 whole annulus blade rows with 93.8M grid points. There have been limited efforts however, to couple it subsequently to turbomachinery CSD, see Doi [98]. Successful coupling with CSD was carried out later at the University of Maryland for helicopter main rotor loads and acoustics prediction (see section on rotorcraft aeroelasticity).

Researchers have tried applying large scale NS CFD, i.e. whole-annulus, multi-blade row, unsteady simulations, to forced response and flutter since the early 2000s. These were uncoupled simulations — either predefined blade motions were prescribed to CFD to study the flow distortions [99, 100, 101], or CFD calculated flow distortions were imposed on the structure to calculate blade deformations [102, 103]. The first procedure can be used for an approximate determination of flutter. The second procedure can be used for an approximate determination of forced response. The first procedure exploits the assumption that flutter in turbomachinery is predominantly a SDOF phenomena. Thus prescribing the torsion mode (or bending mode for supersonic flutter) at its natural frequency, and then integrating blade airloads over each cycle to calculate damping is accepted as a reasonable approach.

Pioneering work on coupled analysis began during the 1990s used frequency domain coupling, see for example Williams et al. [104] for panel solvers, and Gerolymos [105] for Euler solvers. In the work by Gerolymos, the structural dynamics (for a particular mode) was solved in the frequency domain. The periodic response was then transferred to the 3-D Euler solver. The Euler solver was marched in time domain, until periodicity. This cycle of periodic CSD and time domain CSD was repeated until convergence. Note that this approach, if applied to a helicopter rotor, will lead to rapid divergence. A similar method, but with a key innovation, is used in helicopter rotors. This method, termed the delta method, is discussed later in the section on rotary wing aeroelasticity.

Time domain coupling using staggered algorithms began to be applied in the 2000s with single sector calculations for a single blade-row. Carsten et al. [106] have systematically compared predicted modal decay between the time domain and frequency domain solvers in the

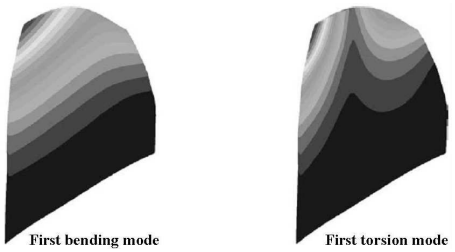

(a) The first bending and first torsion eigenmodes

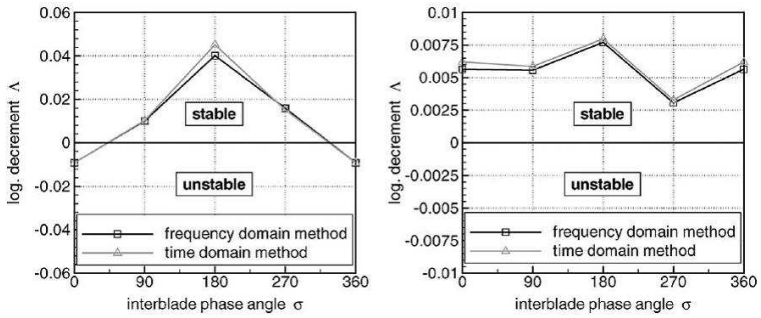

(b) Comparison of logarithmic decrement for frequency and time domain method, first bending(left) and first torsion(right)

Figure 25: **RANS/FEM flutter calculations for a 4-bladed segment of a low pressure compressor annulus using 5 structural modes (20 modes in total); 8 Pentium-4 CPUs; Carsten et al. 2003**

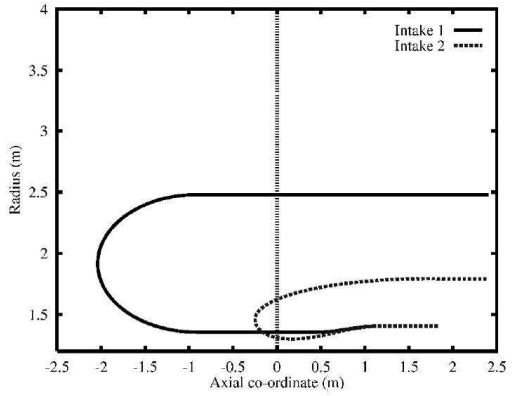

(a) Comparison of two fan intake geometries

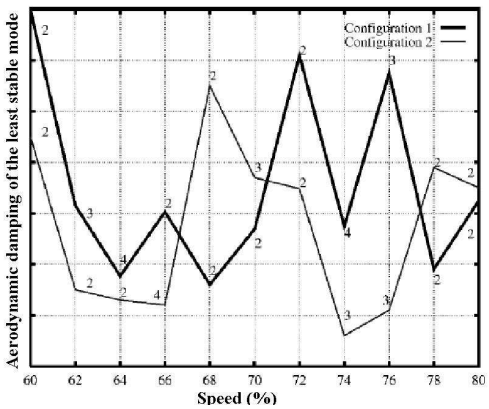

(b) Least stable mode vs % speed

Figure 26: **A RANS/FEM study of intake duct effects on fan flutter stability; Vahdati et al. 2002**

presence of oscillating shocks. For the conditions studied no significant differences were found, as shown in Fig. 25. Whole annulus calculations have been performed extensively by researchers at the Imperial College, London. The original work by Imregun et al. [107, 108] showed that forced vibration predictions remained unchanged between a typical sector analysis (even with adjustment of blade numbers) and whole annulus calculations, as long as multi blade row interactions were not important. Subsequent work by Sayma et al. [109], Breard et al. [110], and Vahdati et al. [111] focused on multi blade row simulations. The last study showed the impact of intake duct geometry on the flutter stability of inlet fans, see Fig. 26. Flutter and forced response calculations for core compressors are more involved, compared to fan flutter, because of the close spacing of blade rows. Rotor-stator blade row interactions involve multiple upstream and downstream rows. In 2005, Wu et al [112] demonstrated the initial feasibility of a massive RANS simulation (Baldwin-Barth turbulence model) including 17 blade rows, see Fig. 27(a). It was performed on 128 CPUs on SGI Origin 3000 with a relatively coarse (compared to the expected requirements) grid of 68M points. A more detailed study on a 5 blade row model was carried out recently by Vahdati et al. [113], see Figs. 27(b) and 27(c). The structural model in all of the above studies was elementary in comparison to CFD. Only rotors 1 and 2 were modeled, and only the 1st flap and 1st torsion modes (of various nodal diameter families) were considered.

Fleeter and his co-researchers have performed fully coupled FEM based CFD/CSD simulations of turboma-

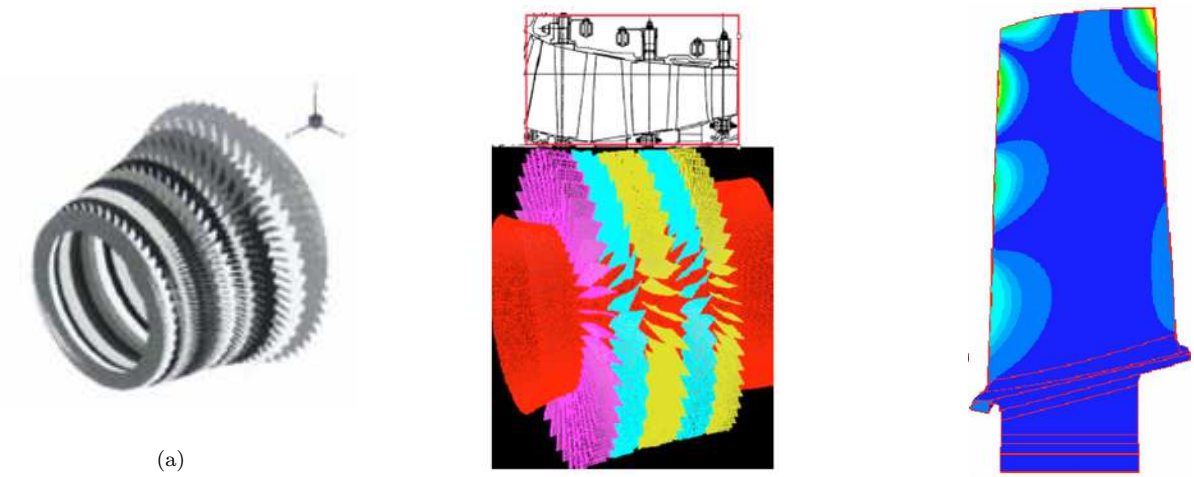

(a) (b) (c)

Figure 27: **A HPC based Whole-annulus, multi blade row aeroelastic analysis of axial-flow compressors using unstructured RANS / FEM coupling; (a) A core-compressor coarse 17 blade row mesh; (b) A refined 5 blade row mesh; (c) Structural mode 11, susceptible to 32nd engine order excitation; Wu et al. 2005; Vahdeti et al. 2007**

chinery flows both for flutter [114] and for forced response [115]. The latter work involved the vibratory stress predictions of a 1.5-stage axial flow compressor (Purdue Transonic Compressor) for a inlet guide vanes-rotor-stator configuration of 18-19-18 blades. Only the rotor and stator were modeled. One segment from each blade row was placed in one CPU. The steel stator vanes were modeled using 2464 hexahedral brick finite elements, 4 across chord and 14 across span. The third mode frequency was 5203 Hz, close to the part-speed blade passage frequency of 4750 Hz (part-speed operating RPM is 15,000, number of blades 19). A simulation was performed at 5203 blade passage frequency (with RPM 16,430). First, the unsteady periodic flow of the rotor was calculated. This required 31 rotor revolutions (80h of CPU time on 2 IBM SP2 processors). The stator vanes were not allowed to deform during this time. This was an aerodynamic only simulation for which a large time step (3844 per period) could be taken. Next, the fully coupled transient fluid-structure simulation was initiated. For this case, the time step was reduced by three times. The solution was marched until steady state periodic conditions. This required 700h of CPU time on 2 IBM-SP2 processors.

ROTARY WING AIRCRAFT

A recent review of rotary wing CFD/CSD, detailing the historical evolution and current status of airloads and structural loads prediction as of 2006, can be found in Datta et al. [116]. The following sections present a summary of that review. In addition, the reader is brought up to date with the latest developments.

As before, the focus here is on CSD, and coupled high-fidelity CFD/CSD methods. A thorough review of rotorcraft CFD methods, from its early inception to its evolution into its present status to future challenges, can be found in Strawn et al. [117] in 2007. As before, the review is divided into two sections. The first section summarizes the status of detailed CSD. The second section summarizes the key aeroelastic phenomena, and the status of CFD/CSD in predicting them.

Structural Modeling

The non-linear coupled PDEs of rotating blade dynamics were systematically derived in the 1970s by several researchers, notably Hodges and his co-researchers [118, 119], Kvaternik et al. [120], and Rosen and Friedmann [121]. The rotor blade was treated as isotropic and straight Euler-Bernoulli beams. By retaining the second-order effects of elastic motion in the kinetic and strain energy terms, and by adding the nonlinearities (up to second order) in extension and torsion produced by bending, 'almost-exact' beam models can be developed. For larger bending deformations, the nonlinearities can be handled by using the 'geometrically exact' beam theories [122], or within a multibody type formulation [123] which allow both rigid and elastic motion of

structural components.

Since the mid 1980s, there was an emphasis on improving cross-section analyses to account for anisotropy produced by composite materials. Research in composite blade modeling has been reviewed in detail by several researchers, most recently by Friedmann in 2004 [124]. The basic idea has been to perform a linear or non-linear two-dimensional cross-sectional analysis, uncoupled from the 1D non-linear beam theories mentioned above, with the goal of obtaining the cross-sectional elastic constants and warping. It has been shown using asymptotic methods that such uncoupling assumptions hold true in most cases for rotor blades [125]. The cross-sectional elastic constants defining the stress-strain relation are however fully coupled. For low frequency dynamic behavior, a classical analysis with a single shear strain measure (as in the case of isotropic beams) can be reasonably accurate, as long as the coupled elastic constants are calculated properly [126]. For higher accuracy, as required for rotor analysis, the strain vector can include two additional strains to account for the transverse shears, or one additional strain to account for the Vlasov or restrained warping. The accuracy of the model depends more on the accuracy of the elastic constants than the number of strain measures. There are several methods for extracting these constants. They are: engineering methods that work well for certain type of cross-sections [127], asymptotic methods which yield closed form solutions for thin walled beams [128, 129], and finite element methods. The latter can be based either on St. Venant's principle [130] or on asymptotic methods [131]. The latter reference provides a generalized treatment, where the cross-sectional equations and the one dimensional blade equations are rigorously deduced from three-dimensional elasticity theory. These analyses or static measurements are used today to obtain the section properties required to operate a beam-theory based comprehensive code. The dynamics of the blade is then calculated, subject to proper modeling of the boundary conditions. The latter is a challenging task because of nonlinearities associated with the root end of the blades, the prime examples of which are lag dampers and control systems.

Gandhi and Chopra [132] incorporated an analytical elastomeric lag damper model in a rotor comprehensive analysis. Finite element based damper models have also been developed, such as by Smith et al [133]. In general, the difficulties with modeling lag dampers are numerous. Non-linearities associated with temperature, amplitude, and frequency of these structures create unknown parameters and reduce prediction accuracy of the blade models. Complex boundary conditions can be handled in a generalized manner using a multibody formulation [134]. Originally developed for spacecraft dynamics, it provides a framework to treat rigid and flexible structural elements undergoing arbitrary rotations and translations with respect to one another. In addition, unlike conventional formulations, multibody formulations enable the increase in scope of analysis without having to re-derive and revalidate the equations with each additional feature. One of the early rotor aeromechanical stability analysis developed to represent arbitrary rigid and flexible dynamics was GRASP by Hodges et al. [135]. This multibody like analysis was designed to treat modern rotors with arbitrary boundary conditions in steady, axial flight and ground contact conditions. Multibody formulations enable large deformation problems to be accurately treated while still retaining second-order nonlinear beam theory (i.e., without using geometrically exact theories). This is done by simply breaking up the rotor blade into multiple bodies each undergoing only moderate deformations in its local frame. The total deformation is obtained by adding the local deformations to the end contribution of the adjoining parent element as a rigid motion.

DYMORE [136] and MBDyn [137] are examples of modern multibody structural codes. These codes are often geared to solve the full non-linear finite element equations using time-marching schemes. This is due to the presence of algebraic constraint equations. Time marching schemes are less suitable for rotor trim. Artificial damping is often required to suppress the natural response of the lowly damped modes, particularly the lag mode. The damping needs to be subsequently removed as the solution progresses to arrive at the correct steady state periodic response. In addition, the use of algebraic equations prevents the use of state space based aeroelastic stability analysis. The accuracy of blade loads prediction, however, have not shown any significant improvement, so far, with the expansion of the scope of structural modeling. The importance of detailed boundary condition modeling, and their impact on the current deficiencies in blade loads prediction, remains to be understood.

The development of coupled rotor-fuselage dynamic analysis can be traced back to the early work of Gerstenberger and Wood [138] in 1963. The work was based on a method of impedance matching, which was later used extensively during the 1970s and 80s [139, 140, 141, 142]. Beginning 1984, NASA Langley Research Center carried out a successful Design Analysis Methods for Vibrations (DAMVIBS) program, with the active participation of four major rotorcraft manufacturers (Bell, Boeing, the former McDonnell-Douglas, and Sikorsky). As part of the program detailed FEM of several metal and composite helicopter fuselages were constructed, e.g. the AH-1G, Model 360, AH-64A, OH-6A, CH-47D, S75, D292, and the UH-60A. An overview of the program can be found in Kvaternik [143]. The description of the airframe FEM models as developed by each of the companies can be found in Refs. [144, 145, 146, 147]. The prevalent

methods of rotor-fuselage dynamic analysis were summarized by Kvaternik et al. [148].

During the 1990s, iterative or fully coupled formulations began to be applied to the rotor-fuselage problem. An early work was that of Stephens and Peters [149], followed by Vellaichamy and Chopra [150], and Chiu and Friedmann [151]. During the 2000s, detailed 3-D fuselage FEM models began to be coupled to rotor dynamics using these formulations. Cribbs et al. [152] studied active vibration control techniques in the fixed frame using a MBB BO-105 type four-bladed hingeless rotor helicopter. The DAMVIBS AH-1G fuselage was used by Yeo and Chopra [153] to carry out vibration prediction studies (see Figs. 6 and 7). A similar (to DAMVIBS) SH-60 fuselage was later used by Yang et al. [154], to study the vibration impact of damaged rotors. Bauchau et al. [155] applied the method of component mode synthesis to couple fuselage dynamics to a multibody rotor model.

Except for the two-bladed teetering AH-1G helicopter, the inclusion of fuselage dynamics had a minor effect on the blade loads. Predicted vibration in the fuselage, of course, relies on fuselage dynamics. As mentioned earlier, all of these studies focused on vibratory forcing transmitted via the shaft. The effect of rotor wake impingement were not included.

Aeroelastic Phenomena and CFD/CSD Predictions

In rotary wing aeroelasticity, a first principles solution requires more than CFD and CSD. It requires, in addition, a method for simultaneously predicting the unsteady control pitch angles and aircraft operating states. This is referred to as the Vehicle Flight Dynamics (VFD) problem in this paper. The requirement arises because unlike fixed-wings and turbomachines, the dynamic loads, flutter (flap-lag), and air-resonance characteristics of the rotor blades are coupled inherently and nonlinearly to vehicle dynamics via the control pitch angles prescribed at the blade root.

In steady flight, straight-level or turns, VFD determines the operating state which holds the entire aircraft in equilibrium. The operating state is defined by the rotor/s pitch control angles (only collective in the case of tail rotors), aircraft attitude angles and rates, fuselage properties (aerodynamic interaction, weight-distribution, tail properties and setting, compounding and special configurations). The word 'coupled trim' is used by dynamicists to describe the VFD associated with steady flight. During unsteady flight, VFD is a generalization of coupled trim, and determines the operating state which follows an intended flight dynamics of the aircraft. For a general maneuver, these intended targets can be a prescribed trajectory in space, or a prescribed mean loading schedule (e.g. g-level and a prescribed set of hub roll and pitch moment variation with time). The optimal control problem of determining the control angles based on these intended targets is still beyond state-of-the-art, even with lower order free wake based lifting-line aerodynamic models.

For steady flight, the VFD problem is relatively simple. The trajectory is trivial, and the mean loading schedule can be calculated from first principles using a six DOF equilibrium in level flight, or an eight DOF equilibrium in a most general steady maneuver (a coordinated helical turn). Calculating VFD (or 'coupled trim') is the first step for predicting performance, loads, vibration, stability, and acoustics. An innovative method for simultaneous determination of VFD during CFD/CSD for rotors was described by Tung et al. in 1986 [156]. Referred to in this paper as the 'delta coupling', it has remained the most efficient approach and has been the cornerstone of all current advances in rotorcraft CFD/CSD. The method is also referred to as 'loose coupling', however, it bears no resemblance with CFD/CSD loose coupling in fixed wings, and the confusion is best avoided.

For unsteady maneuvers, the analysis becomes conceptually simpler when the rotor control angles and vehicle dynamics are known. The VFD is then uncoupled from CFD/CSD simulation. Prescribing VFD, either from measured data or from isolated lower order predictions, reduces the CFD/CSD problem to a straightforward, partitioned, numerical integration problem, similar to those applied in fixed wing and turbo machinery disciplines. Except that, in rotorcraft, the problem is currently solved at a much lower fidelity compared to the other disciplines. First, the structural model for an isolated rotor blade is almost always a beam, compared to 3-D structures in other disciplines. Second, the emphasis in rotors has been on blade loads, not flutter, and therefore errors in approximate fluid-structure coupling methods and low-order (below second order) temporal integration have been of lesser consequence. There is only a single example of CFD/CSD coupling performed so far (see later) for a realistic unsteady maneuver.

The application of delta coupling during the 1990s yielded limited payoffs compared to lifting-line methods [157, 158, 159]. A comprehensive report on loads prediction for the Research Puma helicopter using U.S. and European CFD/CSD methods of the time is documented in Bousman et al. [160] in 1996. Philippe [161], in 1994, presented a summary of other European efforts. The key drawback at the time was the lack of consistent coupling due to the inability of the CFD solvers in resolving the grid and compressibility effects. Renewed interest in the 2000s was spurred by the emergence of reliable unsteady Euler/RANS solvers.

The resurgence of rotary wing CFD/CSD/VFD, in the U.S., stems from the systematic work of Datta et al. [162, 163] and Potsdam et al. [164]. The advances were enabled in substantial part by the reliable and repeatable flight test data provided by the NASA/Army UH-60A Airloads Flight Test Program. Reference [162] dissected the coupled aeroelastic loads problem into aerodynamic, structural dynamic, and trim components; identified the key mechanisms of rotor vibration at high speed, isolated the effects of wake and transonic pitching moments, and clarified the key contribution of Euler/RANS over lifting-line models. Reference [163] brought the components back together again and demonstrated improved airloads and structural loads prediction using CFD/Comprehensive Analysis coupling. The predictions were compared systematically between lifting-line airloads, CFD airloads, and measured airloads. The CFD airloads were computed using near blade RANS coupled to free-wake inflow using the field velocity approach by Sitaraman and Baeder [165].

Potsdam et al. [164] focused on airloads. However, the work extended RANS capabilities beyond the high speed flight to a wake dominated transition flight and a stall dominated highly loaded flight. In the wake dominated flight, the work demonstrated that CFD is capable of predicting the dominant wake induced vibratory airloads at transition speeds even without fully capturing the individual vortices in the wake. At the dynamic stall flight, the work demonstrated that a one equation turbulence model (Baldwin-Barth) is adequate for predicting the basic stall phenomena on the retreating side. The stall flight was subsequently studied in detail by Datta and Chopra [166], isolating the physics of structural dynamics, wake, stall, and trim. The physics of the stall mechanisms and their impact on predicted pitch-link loads using CFD/Comprehensive Analysis coupling were clarified. The CFD analysis used in references [162, 163, 166] was subsequently extended to include overset capabilities for wake capture, similar to that of reference [164], by Duraisamy and Baeder [167]. This methodology was then used to carry out predictions of vibratory airloads and structural loads at all three level flight conditions in Refs. [168, 169]. The work of Potsdam et al. [164] was subsequently extended by Lim et al. [170] for studying vortex loadings in more details. The focus was on descent flights of the UH-60A and HART II rotor where, both the vortex induced loadings as well as the individual BVIs are present in the airloads. The BVI airloads predicted by CFD were improved compared to lifting-line predictions. A significant portion of the improvement was in low frequency harmonics (3/rev), brought about by vortex loadings in the first and fourth quadrants, rather than individual BVI. Increasing the background grid resolution from 10% chord to 5% chord, a difference of 19.4M and 107.6M grid points, did not show any improvement in the individual BVI loadings.

Concurrent developments in Europe over the last five years have also contributed to the increased understanding of CFD/Comprehensive Analysis capabilities for loads prediction in helicopter rotors. The high speed wind tunnel test airloads of the ONERA 7A and 7AD rotors have been studied and predicted by several researchers, see Servera et al. [171], Altmikus et al [172], Pomin and Wagner [173], and Pahlke and Van Der Wall [174]. A discussion on the key accomplishements in all of the above work can be found in the review article, Ref. [116].

The developments cited above provided a renewed impetus for integrating CFD reliably within the rotor design process. At the time, among all key design issues, noise, tied directly to vulnerability, was considered to be of immediate urgency. Innovative blade shapes and advanced blade geometries for noise reduction are not considered as serious contenders for blade design because their impact on performance, loads, and vibration cannot be predicted with confidence. As CFD begins to predict the fundamental mechanisms for structural loads — 3-D unsteady transonic pitching moments, wake induced airloads and BVI, and dynamic stall cycles — a considerable attention is now focused on increasing CFD throughput while maintaining the same level of accuracy as benchmarked by the above cited works. The DARPA Helicopter Quieting Program was designed to carry out such a task. A key objective of the DARPA program was to adapt non-rotorcraft CFD with demonstrated scalability to rotor airloads prediction. For example, the TFLOW2000 code was adapted for rotary wing CFD (extended and renamed SUmb) and coupled to a rotorcraft comprehensive analysis, as part of the program. An additional objective of the program was to investigate the impact of high fidelity wake and turbulence modeling, e.g. methods for solution adaptive background mesh refinements, different near-blade and background solvers, and v^2-f and KES turbulence models, which these analyses incorporated. The focus was not on CSD or coupling methods. To this end, trimmed aeroelastic blade deformations from Ref. [164], were supplied to the participants as an initial step. As a follow on, the participants performed the same CFD/CSD/VFD coupling as in Refs. [163, 164] using the same comprehensive analysis tools. The validation set was extended to include acoustic signatures in addition to performance and airloads. The DNW model UH-60A, and the BO-105 model HART-II rotor were considered as validation cases for acoustics. The contributions of the three program participant teams are partially documented in Refs. [176, 177, 178, 179].

All of the above coupled studies, with the exception

of reference [173], used variations of the delta coupling method in the time domain. Reference [173] does not calculate control angles as part of the CFD coupled solution but determines them a priori using an uncoupled lifting-line comprehensive analysis. The delta method is unique to rotorcraft and is not found in fixed-wing or turbomachinary aeroelasticity. It accounts for the following key requirements of rotor CSD: (1) it operates, by design, at or near resonance in flap, (2) it requires simultaneous solution of VFD for the pitch control angles. The description of the original method can be found in Ref. [156], its current adaptations in any of the above references, see for example Refs. [164, 163]. The method is implied in rotorcraft literature by the frequent use of the term 'CFD/Comprehensive Analysis'. The term 'Comprehensive Analysis', by itself, historically refers to a complete analysis, which contains within itself all of the airloads, structural loads, and VFD models. Thus, 'CFD/Comprehensive Analysis' simply refers to a CFD/CSD/VFD analysis which uses the CSD and VFD of existing comprehensive analysis while replacing the built-in lifting-line/surface aerodynamics with CFD via the delta coupling method.

In the special case where the control angle variation is assumed to be known a priori, either from measured test data or from separate uncoupled estimates from lower order models, the problem reduces to a pure CFD/CSD analysis. A straight-forward, partitioned, numerical integration procedure can then be applied, similar to those used in fixed-wing or turbomachinery. Except that, for an isolated rotor analysis, the problem is rendered much simpler as the structural model is almost always a beam, and a low order fluid-structure interface is much simpler to devise. These methods are known was 'tight coupling' in rotorcraft. Again, note the confusing nomenclature as compared to fixed wing terminology. In fixed wing tight coupling implies strict time accuracy via sub-iterations. One of the first implementations of tight coupling in rotorcraft using RANS CFD was by Bauchau and Ahmad [180]. Recent studies are those of Pomin and Wagner [173] and Bhagwat et al [181]. The latter work is of significance as it is the first application of CFD to a real unsteady maneuver. The method is applied here to a pull-up maneuver, the second most severe (loads) of the UH-60A maneuvers. Note that, the advances in this study were enabled by the NASA/Army UH-60A Airloads Flight Test Program Data. The rotor control angles and vehicle dynamics were prescribed from measured flight data. Several key conclusions can be drawn from this work. First, it demonstrates RANS capability for predicting advancing blade transonic stall. Second, it appears to negate the role of fuselage upwash on rotor stall and pitch-link loads during a pull-up maneuver. Third, it demonstrates that an isolated rotor calculation can predict the oscillatory (peak-to-peak) control loads correctly in the severest of the UH-60A maneuvers.

A LIST OF TEMPORAL COUPLING PROCEDURES

In view of the conflicting nomenclatures often used across disciplines to describe the various methods of temporal coupling, a list is summarized below.

1. *Loose coupling*: Partitioned formulation based temporal advancement, but without sub-iterations. Predictor-corrector schemes often used to seek near-second order accuracy. Standard nomenclature in fixed wing. Described as tight coupling in rotary wing.

2. *Tight coupling*: Partitioned formulation based time advancement, but with sub-iterations. Temporal accuracy level of worse solver. Standard nomenclature in fixed wing. Also called *close coupling* or *strong coupling*.

3. *Periodic coupling*: For periodic dynamics. First applied by Gerolymos for turbomachinery. Iterates on harmonics of loads and deformations. Strict time accuracy can be enforced on any chosen set of harmonics.

4. *Delta coupling*: Periodic coupling with the use of aerodynamic damping from lower order models. Only successful approach for CFD/CSD/VFD in rotorcraft. Conflictingly nomenclature as *loose coupling* in rotary wing. Note, not *loose* in the fixed wing sense of the term. Strict time accuracy can be enforced on any chosen set of harmonics.

5. *Full coupling*: Formulation coupled via boundary conditions (deflection and velocity compatibility, and stress equilibrium) and integrated together. Also called *direct coupling*, *intimate coupling*, or *monolithic coupling*.

CONCLUDING OBSERVATIONS

The objective of the present paper was to motivate research towards the next generation HPC based high-fidelity rotorcraft comprehensive analysis. To this end, the frontiers of fixed wing, turbomachinery, and rotary wing aeroelasticity were reviewed, along with a survey of the fluid-structure coupling methodologies used in each. The underlying theme of the paper was rotorcraft. Therefore, the technology areas in each discipline were tied to the future rotorcraft requirements, where deemed relevant by the authors. In addition, comparisons were drawn between the computational procedures

used in each of the disciplines, and those required by the unique rotorcraft requirements.

CFD is only one part of a next generation comprehensive analysis. The ultimate objective of reliably discriminating between innovative blade shapes, rotor types, and rotor-fuselage configurations, requires CFD, CSD, high-fidelity coupling, and a solution procedure that ties CFD/CSD to VFD satisfying the unique operating principles of rotorcraft. The focus so far has largely been on CFD. This is because CFD, up to recently, was unable to meet the fundamental requirements for vibratory structural loads in rotorcraft: predicting transonic pitching moments on blades, wake induced airloads on both blades and fuselage, dynamic stall cycles on blades, and buffet loads on the fuselage driven by massive separation. HPC based CFD is now beginning to address these requirements. The methods of high-fidelity CSD, fluid-structure coupling, and solution procedures must now be re-evaluated and re-shaped for taking rotorcraft comprehensive analysis to the next level.

REFERENCES

[1] Johnson, W., and Datta, A., "Requirements for Next Generation Comprehensive Analysis of Rotorcraft," American Helicopter Society Specialist's Conference on Aeromechanics, San Francisco, CA, January 23-25, 2008.

[2] Kilic, S. A., Saied, F., and Sameh, A., "Efficient Iterative Solvers for Structural Dynamics Problems," *Computers and Structures*, Vol. 82, (28), November 2004, pp. 2363–2375.

[3] Gottfried, D. A., and Fleeter, S., "Turbomachine Blade Row Interaction Predictions with a Three-Dimensional Finite Element Method," *Journal of Propulsion and Power*, Vol. 18, (5), September-October 2002, pp. 978–989.

[4] Bathe, K. and Zhang, H., "Finite Element Developments for General Fluid Flows with Structural Interactions," *International Journal for Numerical Methods in Engineering*, Vol. 60, (1), May 2004, pp. 213–232.

[5] Hirt, C. W., Amsden, A. A., and Cook, J. L., "An Arbitrary Lagrangian-Eulerian Computing Method for All Flow Speeds," *Journal of Computational Physics*, Vol. 14, 1974, pp. 227–253.

[6] Donea, J., "Arbitrary Lagrangian-Eulerian Finite Element Methods,", Computational Methods for Transient Analysis, eds. Belytschko, T., and Hughes, T. J. R., North-Holland, Amsterdam, 1983, pp. 473–516.

[7] Bendiksen, O. O., "A New Approach to Computational Aeroelasticity," Paper AIAA 91-0939.

[8] Bendikson, O. O., "Eulerian-Lagrangian Simulations of Transonic Flutter Instabilities," *Aeroelasticity and Fluid Structure Interaction Problems*, Vol. 44, Aerospace Division, ASME, Fairfield, NJ, 1994, pp. 197–231.

[9] Strganac, T. W., and Mook, D. T., "Numerical Model of Unsteady Subsonic Aeroelastic Behavior," *AIAA Journal*, Vol. 28, (5), May 1990, pp. 903–909.

[10] Pramono, E., and Weeratunga, S., "Aeroelastic Computations for Wings Through Direct Coupling on Distributed-memory MIMD Parallel Computers," Paper AIAA 1994-95, Aerospace Sciences Meeting and Exhibit, 32nd, Reno, NV, January 10–13, 1994.

[11] Morton, S. A., Melville, R. B. and Visbal, M. R., "Accuracy and Coupling Issues of Aeroelastic Navier-Stokes Solutions of Deforming Meshes," Paper AIAA 97-1085, AIAA/ASME/ASCE/AHS/ASC Structures, Structural Dynamics, and Materials Conference and Exhibit, 38th, and AIAA/ASME/AHS Adaptive Structures Forum, Kissimmee, FL, April 7-10, 1997.

[12] Gordnier, R. E., and Melville, R. B., "Transonic Flutter Simulations Using an Implicit Aeroelastic Solver," *Journal of Aircraft*, Vol. 37, (5), September-October 2000, pp. 872–879.

[13] Edwards, J. W., Bennett, R. M., Whitlow, W., Jr., and Seidel, D. A., "Time-Marching Transonic Flutter Solutions Including Angle-of-Attack Effects," *Journal of Aircraft*, Vol. 20, (11), November 1983, pp. 899–906.

[14] Bennett, R. M., Batina, J. T., and Cunningham, H. J., "Wing-Flutter Calculations with the CAP-TSD Unsteady Transonic Small-Disturbance Program," *Journal of Aircraft*, Vol. 26, (9), September 1989, pp. 876–882.

[15] Guruswamy, P. and Yang, T. Y., "Aeroelastic Time-Response Analysis of Thin Airfoils by Transonic Code LTRAN2," *Computers and Fluids*, Vol. 9, (4), December 1980, pp. 409–425.

[16] Guruswamy, G. P., "Unsteady Aerodynamic and Aeroelastic Calculations for Wings Using Euler Equations," *AIAA Journal*, Vol. 28, (3), March 1990, pp. 461–469.

[17] Farhat, C. and Lesoinne, M., "Two Efficient Staggered Algorithms for The Serial and Parallel Solution of Three-Dimensional Nonlinear Transient Aeroelastic Problems," *Computer Methods in Applied Mechanics and Engineering*, Vol. 182, (3-4), February 2000, pp. 499–515.

[18] Farhat, C., Van der Zee, K. G., and Geuzaine, P., "Provably Second-Order Time-accurate Loosely-coupled Solution Algorithms for Transient Nonlinear Computational Aeroelasticity," *Computer Methods in Applied Mechanics and Engineering*, Vol. 195, (17-18), March 2006, pp. 1973–2001.

[19] Maman, N. and Farhat, C., "Matching Fluid and Structure Meshes for Aeroelastic Computations: A Parallel Approach," *Computers and Structures*, Vol. 54, (4), 1995, pp. 779–785.

[20] Cebral, J. R., and Lohner, R., "Conservative Load Projection and Tracking for Fluid-Structure Problems," *AIAA Journal*, Vol. 35, (4), 1997, pp. 687–692.

[21] Farhat, C., Lesoinne, M. and LeTallec, P., "Load and Motion Transfer Algorithms for Fluid/Structure Interaction Problems with Non-matching Discrete Interfaces: Momentum and Energy Conservation, Optimal Discretization and Application to Aeroelasticity," *Computer Methods in Applied Mechanics and Engineering*, Vol. 157, (1), April 1998, pp. 95–114.

[22] Slone, A. K., Pericleous, K., Bailey, C. and Cross, M., "Dynamic Fluid-Structure Interaction Using Finite Volume Unstructured Mesh Procedures," *Computers and Structures*, Vol. 80, (5), March 2002, pp. 371–390.

[23] Michler, C., Van Brummelen, E. H., Hulshoff, S. J. and De Borst, R., "The Relevance of Conservation for Stability and Accuracy of Numerical Methods for Fluid-Structure Interaction," *Computer Methods in Applied Mechanics and Engineering*, Vol. 192, (37), September 2003, pp. 4195–4215.

[24] Brown, R. E. and Line, A. J., "Efficient High-resolution Wake Modeling Using the Vorticity Transport Equation," *AIAA Journal*, Vol. 43, (7), July, 2005, pp. 1434–1443.

[25] Whitehouse, G. R., Boschitsch, A. H., Quackenbush, T. R., Wachspress, D. A., and Brown, R. E., "Novel Eulerian Vorticity Transport Wake Module for Rotorcraft Flow Analysis," American Helicopter Society 63rd Annual Forum Proceedings, Virginia Beach, May 1–3, 2007.

[26] Fasanella, E. L., Jackson, K. E., Lyle, K. H., Sparks, C. E., Sareen, A. K., "Multi-Terrain Impact Tests and Simulations of an Energy Absorbing Fuselage Section," *Journal of the American Helicopter Society*, Vol. 52, (2), April 2007, pp. 159–167.

[27] Hounjet, M. H. L. and Meijer, J. J., "Evaluation of Elastomechanical and Aerodynamic Data Transfer for Non-Planar Configurations in CAE Analysis," Proceedings of the International Forum on Aeroelasticity and Structural Dynamics, Manchester, UK, published by the Royal Aeronautical Society, pp. 10.1–10.25.

[28] Smith, M. J., Hodges, D. H., and Cesnik, C. E. S., "Evaluation of Computational Algorithms Suitable for Fluid-Structure Interactions," *Journal of Aircraft*, Vol. 37, (2), March–April 2000, pp. 282–294.

[29] Goura, G. S. L., Badcock, K. J., Woodgate, M. A., and Richards, B. E., "A Data Exchange Method for Fluid-Structure Interaction Problems," *The Aeronautical Journal*, Vol. 105, (1046), April 2001, pp. 215–221.

[30] Goura, G. S. L., Badcock, K. J., Woodgate, M. A., and Richards, B. E., "Extrapolation Effects on Coupled Computational Fluid Dynamics/Computational Structural Dynamics Simulations," *AIAA Journal*, Vol. 42, (2), June 2003, pp. 312–315.

[31] Chen, P. C., and Jadic, I., "Interfacing of Fluid and Structural Models via Innovative Structural Boundary Element Method," *AIAA Journal*, Vol. 36, (2), February 1998, pp. 282-287.

[32] Wu, Z., "Compactly supported positive definite radial functions," *Advances in Computational Mathematics*, Vol. 4, (3), 1995, pp. 283–292.

[33] Wendland, H., "Piecewise Polynomial, Positive Definite and Compactly Supported Radial Functions of Minimal Degree," *Advances in Computational Mathematics*, Vol. 4, (1), December 1995, pp. 389–396.

[34] Beckert, A., and Wendland, H., "Multivariate Interpolation for Fluid-Structure-Interaction Problems Using Radial Basis Functions," *Aerospace Science and Technology*, Vol. 5, (2), February 2001, pp. 125–134.

[35] Ahrem, R., Beckert, A., and Wendland, H., "A Meshless Spatial Coupling Scheme for Large-Scale Fluid-Structure-Interaction Problems," *Computer Modeling in Engineering and Sciences*, Vol. 12, (2), 2006, pp. 121–136.

[36] Rendall, T. C. S., and Allen, C. B., "Unified Approach to CFD-CSD Interpolation and Mesh Motion Using Radial Basis Functions," Paper AIAA 2007-3804, AIAA Applied Aerodynamics Conference, 25th, Miami, June 25-28, 2007.

[37] Livne, E., "Future of Airplane Aeroelasticity," *Journal of Aircraft*, Vol. 40, (6), November–December 2003, pp. 1066–1092.

[38] Schuster, D. M., Liu, D. D. and Huttsell, L. J., "Computational Aeroelasticity: Success, Progress, Challenge," *Journal of Aircraft*, Vol. 40, (5), September–October 2003, pp. 843–856.

[39] Kamakoti, R. and Shyy, W., "Fluid-Structure Interaction For Aeroelastic Applications," *Progress in Aerospace Sciences*, Vol. 40, 2004, pp. 535–558.

[40] Bartels, R. E. and Sayma, A. I., "Computational Aeroelastic Modeling of Airframes and Turbomachinery: Progress and Challenges," *Philosophical Transactions of The Royal Society: Mathematical, Physical and Engineering Sciences*, Vol. 365, (1859), October 2007, pp. 2469–2499.

[41] Henshaw, M. J. de C., Badcock, K. J., Vio, G. A., Allen, C. B., Chamberlain, J., Kaynes, I., Dimitriadis, G., Cooper, J. E., Woodgate, M. A., Rampurawala, A. M., Jones, D., Fenwick, C., Gaitonde, A. L., Taylor, N. V., Amor, D. S., Eccles, T. A. and Denley, C. J., "Non-linear Aeroelastic Prediction For Aircraft Applications," *Progress in Aerospace Sciences*, Vol. 43, 2007, pp. 65–137.

[42] van Dam, C. P., "The Aerodynamic Design of Multi-element High-lift Sytems for Transport Airplanes," *Progress in Aerospace Sciences*, Vol. 38, (2), February 2002, pp. 101–144.

[43] Mohaghegh, M., "Evolution of Structures Design Philosophy and Criteria," *Journal of Aircraft*, Vol. 12, (4), July-August 2005, pp. 814–831.

[44] Yurkovich, R., "Status of Unsteady Aerodynamic Prediction for Flutter of High-Performance Aircraft," *Journal of Aircraft*, Vol. 40, (5), pp.832–842.

[45] Melville, R., "Nonlinear Simulation of F-16 Aeroelastic Instability," Paper AIAA 2001-0570, AIAA Aerospace Sciences Meeting and Exhibit, 39th, January 8-11, Reno, NV, 2001.

[46] Melville, R., "Nonlinear Mechanisms of Aeroelastic Instability For the F-16," Paper AIAA 2002-0871, AIAA Aerospace Sciences Meeting and Exhibit, 40th, January 14-17, Reno, NV, 2002.

[47] Denegri, C. M., "Limit Cycle Oscillation Flight Test Results of a Fighter With External Stores," *Journal of Aircraft*, Vol. 37, (5), September-October 2000, pp. 761–769.

[48] Morton, S. A., Melville, R. B. and Visbal, M. R., "Accuracy and Coupling Issues of Aeroelastic Navier-Stokes Solutions on Deforming Meshes," *Journal of Aircraft*, Vol. 35, (5), September-October, 1998, pp. 798–805.

[49] Geuzaine, P., Brown, G., Harris, C., and Farhat, C., "Aeroelastic Dynamic Analysis of a Full F-16 Configuration for Various Flight Conditions," *AIAA Journal*, Vol. 41, (3), March 2003, pp. 363–371.

[50] Farhat, C., Geuzaine, P. and Brown, G., "Application of a Three-Field Nonlinear Fluid-Structure Formulation to the Prediction of The Aeroelastic Parameters of an F-16 Fighter," *Computers and Fluids*, Vol. 32, 2003, pp. 3–29.

[51] Lieu, T. and Farhat, C., "Adaptation of Aeroelastic Reduced-Order Models and Application to an F-16 Configuration," *AIAA Journal*, Vol. 45, (6), June 2007, pp. 1244–1257.

[52] Hong, M. S., Bhatia, K. G., SenGupta, G., Kim, T., Kuruvila, G., Silva, W. A., Bartels, R. and Biedron, R., "Simulations of a Twin-Engine Transport Flutter Model in the Transonic Dynamics Tunnel," International Forum on Aeroelasticity and Structural Dynamics, June 4-6, Amsterdam, The Netherlands.

[53] Kim, T., Hong, M., Bhatia, K. G. and SenGupta, G., "Aeroelastic Model Reduction for Affordable Computational Fluid Dynamics-Based Flutter Analysis," *AIAA Journal*, Vol. 43, (12), December 2005, pp. 2487–2495.

[54] Lee, B. H. K., "Vertical Tail Buffeting of Fighter Aircraft," *Progress in Aerospace Sciences*, Vol. 36, 2000, pp. 193–279.

[55] Rizk, Y. M. and Gee, K., "Unsteady Simulation of Viscous Flowfield Around F-18 Aircraft at Large Incidence," *Journal of Aircraft*, Vol. 29, (6), November-December 1992, pp.986–992.

[56] Ghaffari, F., Luckring, J. M., and Thomas, J. L., "Multiblock Navier-Stokes Solutions about the F/A-18 Wing-LEX-Fuselage Configuration," *Journal of Aircraft*, Vol. 30, (3), May-June 1993, pp.293–303.

[57] Gee, K, Murman, S., and Schiff, L., "Computation of F/A-18 Tail Buffet," *Journal of Aircraft*, Vol. 33, (6), 1996, pp. 1181-1189.

[58] Sheta, E., "Alleviation of Vertical Tail Buffeting of F/A-18 Aircraft," *Journal of Aircraft*, Vol. 41, (2), March-April 2004, pp. 322-330.

[59] Morton, S. A., Cummings, R. M. and Kholodar, D. B., "High Resolution Turbulence Treatment of F/A-18 Tail Buffet," *Journal of Aircraft*, Vol. 44, (6), November-December 2007, pp. 1769–1775.

[60] Pirzadeh, S. Z., "A Solution-Adaptive Unstructured Grid Method by Grid Subdivision and Local Remeshing," *Journal of Aircraft*, Vol. 37, (5), 2000, pp. 818-824.

[61] Bunton, R. W. and Denegri, C. M., "Limit Cycle Oscillation Characteristics of Fighter Aircraft," *Journal of Aircraft*, Vol. 37, (5), September-October 2000, pp. 916–918.

[62] Bendiksen, O. O., "Transonic Limit Cycle Flutter/LCO," Paper AIAA 2004-1694, AIAA/ASME/ASCE/AHS/ASC Structures, Structural Dynamics and Materials Conference, Palm Springs, CA, April 19-22, 2004.

[63] Tijdeman, H. and Seebass, R., "Transonic Flow Past Oscillating Airfoils," *Annual Review of Fluid Mechanics*, Vol. 12, December 1980, pp. 181–222.

[64] Denegri, C. M., Dubben, J. A. and Maxwell, D. L., "In-Flight Wing Deformation Characteristics During Limit-Cycle Oscillations," *Journal of Aircraft*, Vol. 42, (2), March-April 2005, pp. 500–508.

[65] Thomas, J. P., Dowell, E. H. and Hall, K. C., "Virtual Aeroelastic Flight Testing for the F-16 Fighter with Stores," Paper AIAA 2007-1640, U.S. Air Force T&E Days Conference, Destin, FL, February 13-15, 2007.

[66] Parker, G. H., Maple, R. C. and Beran, P. S., "Computational Aeroelastic Analysis of Store-Induced Limit-Cycle Oscillation," *Journal of Aircraft*, Vol. 44, (1), January-February 2007, pp. 48–59.

[67] Beran, P., Khot, N., Eastep, F., Snyder, R. and Zweber, J., "Numerical Analysis of Store-Induced Limit-Cycle Oscillation," *Journal of Aircraft*, Vol. 41, (6), November-December 2004, pp. 1315–1326.

[68] Eastep, F. and Olsen, J. J., "Transonic Flutter Analysis of a Rectangular Wing with Conventional Airfoil Sections," *AIAA Journal*, Vol. 18, (10), October 1980, pp. 1159-1164.

[69] Goland, M., "The Flutter of a Uniform Cantilever Wing," *Journal of Applied Mechanics*, Vol. 12, (4), December 1945, pp. 197–208.

[70] Goodman, C., Hood, M., Reichenback, E., and Yurkovich, R., "An Analysis of the F/A-18C/D Limit Cycle Oscillation Solution," Paper AIAA 2003-1424, AIAA/ASME/ASCE/AHS Structures, Structural Dynamics, and Materials Conference, Norfolk, VA, April 7-10, 2003.

[71] Hartwich, P. M., Dobbs, S. K., Arslan, A. E. and Kim, S. C., "Navier-Stokes Computations of Limit-Cycle Oscillations for a B-1 Like Configuration," *Journal of Aircraft*, Vol. 38, (2), 2001, pp. 239–247.

[72] Jacobson, S. B., Britt, R. T., Dreim, D. R. and Kelly, P. D., "Residual Pitch Oscillation (RPO) Flight Test and Analysis on The B-2 Bomber," Paper AIAA 98-1805.

[73] Mikolajczak, A. A., Arnoldi, R. A., Snyder, L. E., and Stargardter, H., "Advances in Fan and Compressor Blade Flutter Analysis and Predictions," *Journal of Aircraft*, Vol. 12, (4), April 1975, pp. 325–332.

[74] Bendiksen, O. O., "Aeroelastic Problems in Turbomachines," Paper AIAA-90-1157, AIAA/ASME/ASCE/AHS/ASC Structures, Structural Dynamics and Materials Conference, 31st, April 2–4, 1990, Long Beach, CA.

[75] Marshall, J. G. and Imregun, M., "A Review of Aeroelasticity Methods with Emphasis on Turbomachinery Applications," *Journal of Fluids and Structures*, Vol. 10, (3), April 1996, pp. 237–267.

[76] Cumpsty, N. A. and Greitzer, E. M., "Ideas and Methods of Turbomachinery Aerodynamics: A Historical View," *Journal of Propulsion and Power*, Vol. 20, (1), January-February 2004, pp.15–26.

[77] Srinivasan, A. V., "Flutter and Resonant Vibration Characteristics of Engine Blades," *Journal of Engineering for Gas Turbines and Power*, Vol. 119, (4), 1997, pp. 742–775.

[78] Slater, J. C., Minkiewicz, G. R., and Blair, A. J., "Forced Response of Bladed Disk Assemblies - A survey," *Shock and Vibration Digest*, Vol. 31, (1), 1999, pp. 17–24.

[79] Castanier, M. P., and Pierre, C., "Modeling and Analysis of Mistuned Bladed Disk Vibration: Status and Emerging Directions," *Journal of Propulsion and Power*, Vol. 22, (2), March-April 2006, pp. 384–396.

[80] Arakere, N. K., Knudsen, E., Swanson, G. R., Duke, G., and Ham-Battista, G., "Subsurface Stress Fields in Face-Centered-Cubic Single-Crystal Anisotropic

Contacts," *Journal of Engineering for Gas Turbines and Power*, Vol. 128, October 2006, pp. 879–888.

[81] Beisheim, J. R., and Sinclair, G. B., "On the Three-Dimensional Finite Element Analysis of Dovetail Attachments," *Journal of Turbomachinery*, Vol. 125, April 2003, pp. 372–379.

[82] Petrov, E. P., and Ewins, D. J., "Advanced Modeling of Underplatform Friction Dampers for Analysis of Bladed Disk Vibration," *Journal of Turbomachinery*, Vol. 129, January 2007, pp. 143–150.

[83] Petrov, E. P., "Direct Parametric Analysis of Resonance Regimes for Nonlinear Vibrations of Bladed Disks," *Journal of Turbomachinery*, Vol. 129, July 2007, pp. 495–502.

[84] Whitehead, D. S., "Effect of Mistuning on the Vibration of Turbomachine Blades Induced by Wakes," *Journal of Mechanical Engineering Science*, Vol. 8, (1), 1966, pp. 15–21.

[85] Ewins, D. J., "The Effects of Detuning Upon the Forced Vibrations of Bladed Disks," *Journal of Sound and Vibration*, Vol. 9, (1), 1969, pp. 65–79.

[86] Petrov, E. P., and Ewins, D. J., "Analysis of the Worst Mistuning Patterns in Bladed Disk Assemblies," *Journal of Turbomachinery*, Vol.125, October 2003, pp. 623–631.

[87] Rivas-Guerra, A. J., and Mignolet, M. P., "Maximum Amplification of Blade Response due to Mistuning: Localization and Mode Shape Aspects of the Worst Disks," *Journal of Turbomachinery*, Vol. 125, July 2003, pp. 442–454.

[88] Kenyon, J. A., Griffin, J. H., and Kim, N. E., "Frequency Veering Effects on Mistuned Bladed Disk Forced Response," *Journal of Propulsion and Power*, Vol. 20, (5), September-October 2004, pp. 863–870.

[89] Kenyon, J. A., Griffin, J. H., and Kim, N. E., "Sensitivity of Tuned Bladed Disk Response to Frequency Veering," *Journal of Engineering for Gas Turbine and Power*, Vol. 127, October 2005, pp. 835–842.

[90] Bladh, R., Castanier, M. P., and Pierre, C., "Effects of Multistage Coupling and Disk Flexibility on Mistuned Bladed Disk Dynamics," *Journal of Engineering for Gas Turbine and Power*, Vol. 125, January 2003, pp. 121–130.

[91] Wilson, M. J., Imregun, M. and Sayma, A., "The Effect of Stagger Variability in Gas Turbine Fan Assemblies," *Journal of Turbomachinery*, Vol. 129, (2), April 2007, pp. 404–411.

[92] Thomas, D. E., and Griffin, J. T., "The National Turbine Engine High Cycle Fatigue Program," *Global Gas Turbine News*, Vol. 39, (1), 1999, pp. 14–17.

[93] Chen, J. P. and Briley, W. R., "A Parallel Flow Solver for Unsteady Multiple Blade Row Turbomachinery Simulations," *Journal of Turbomachinery*, Vol. 115, (2), 1993, pp. 240–248.

[94] Engel, K., Eulitz, F., Pokorny, S., and Faden, M., "3D Navier-Stokes Solver for the Simulation of the Unsteady Turbomachinery Flow on a Massively Parallel Hardware Architechture," *Notes on Numerical Fluid Mechanics, Vol. 52, Flow Simulation with High-Performance Computers II*, edited by E. H. Hirshel, Springer-Verlag, Berlin, 1996, pp. 117-133.

[95] Jung, A. R., Mayer, J. F., and Stetter, H., "Unsteady Flow Simulation in an Axial Flow Turbine Using a Parallel Implicit Navier-Stokes Method," *High Performance Computing in Science and Engineering '98*, edited by E. J. Krause and W. Jager, Springer-Verlag, Berlin, 1999, pp. 269–294.

[96] Yao, J., Jameson, A., Alonso, J. J., and Liu, F., "Development and Validation of a Massively Parallel Flow Solver for Turbomachinery Flows," *Journal of Propulsion and Power*, Vol. 17, (3), May-June 2001, pp. 659–668.

[97] Yao, J., Davis, R. L., Alonso, J. J., and Jameson, A., "Massively Parallel Simulation of the Unsteady Flow in an Axial Turbine Stage," *Journal of Propulsion and Power*, Vol. 18, (2), March-April 2002, pp. 465–471.

[98] Doi, H., "Fluid/Structure Coupled Aeroelastic Computations for Transonic Flows in Turbomachinery," Ph.D. Thesis, Department of Aeronautics and Astronautics, Stanford University, August 2002.

[99] Silkowski, P. D., Rhie, C. M., Copeland, G. S., Eley, J. A., and Bleeg, J. M., "Computational-Fluid-Dynamics Investigation of Aeromechanics," *Journal of Propulsion and Power*, Vol. 18, (4), July-August 2002, pp. 788–796.

[100] Srivastava, R., Bakhle, M. A., and Keith, T. G. Jr., "Numerical Simulation of Aerodynamic Damping for Flutter Analysis of Turbomachinery Blade Rows," *Journal of Propulsion and Power*, Vol. 19, (2), 2003, pp. 260–267.

[101] Srivastava, R. and Keith, T. G. Jr., "Influence of Shock Wave on Turbomachinery Blade Row Flutter," *Journal of Propulsion and Power*, Vol. 21, (1), January-February 2005, pp. 167–173.

[102] Filsinger, D., Szwedowicz, J., and Schäfer, O., "Approach to Unidirectional Coupled CFD-FEM Analysis of Axial Turbocharger Turbine Blades," *Journal of Turbomachinery*, Vol. 124, January 2002, pp. 125–131.

[103] Moffatt, S., Ning, W., Li Yansheng, Wells, R. G., "Blade Forced Response Prediction for Industrial Gas Turbines", *Journal of Propulsion and Power*, Vol. 21, (4), July-August 2005, pp. 707–713.

[104] Williams, M. H., Cho, J., and Dalton, W. N., "Unsteady Aerodynamic Analysis of Ducted Fans," *Journal of Propulsion and Power*, Vol. 7, (5), 1991, pp. 800–804.

[105] Gerolymos, G. A., "Coupled Three-Dimensional Aeroelastic Stability Analysis of Bladed Disks," *Journal of Turbomachinery*, Vol. 115, (4), October 1993, pp. 791–799.

[106] Carstens, V., Kemme, R., and Schmitt, S., "Coupled Simulation of Flow-Structure Interaction in Turbomachinery", *Aerospace Science and Technology*, Vol. 7, 2003, pp. 298–306.

[107] Sayma, A. I., Vahdati, M., and Imregun, M., "An Integrated Nonlinear Approach for Turbomachinery Forced Response Prediction. Part I: Formulation," *Journal of Fluids and Structures*, Vol. 14, 2000, pp. 87–101.

[108] Vahdati, M., Sayma, A. I., and Imregun, M., " An Integrated Nonlinear Approach for Turbomachinery Forced Response Prediction. Part II: Case Studies," *Journal of Fluids and Structures*, Vol. 14, 2000, pp. 103–125.

[109] Sayma, A. I., Vahdati, M. and Imregun, M., "Multi-bladerow Fan Forced Response Predictions using an Integrated Three-Dimensional Time-domain Aeroelasticity Model," *Proceedings of the Institution of Mechanical Engineers Part C Journal of Mechanical Engineering Science*, Vol. 214, (12), 2000, pp. 1467–1483.

[110] Bréard, C., Vahdati, M., Sayma, A. I., and Imregun, M., "An Integrated Time-Domain Aeroelasticity Model for the Prediction of Fan Forced Response due to Inlet Distortion," *Journal of Engineering for Gas Turbines and Power*, Vol. 124, January 2002, pp. 196–208.

[111] Vahdati, M., Sayma, A. I., Bréard, C., and Imregun, M., "Computational Study of Intake Duct Effects on Fan Flutter Stability," *AIAA Journal*, Vol. 40, (3), March 2002, pp. 408–418.

[112] Wu, X., Vahdati, M., Sayma, A. and Imregun, M., "Whole-Annulus Aeroelasticity Analysis of a 17-Bladerow WRF Compressor Using an Unstructured Navier-Stokes Solver," *International Journal of Computational Fluid Dynamics*, Vol. 19, (3), March 2005, pp. 211–223.

[113] Vahdati, M., Sayma, A. I., Imregun, M. and Simpson, G., "Multirow Forced Response Modeling in Axial-Flow Core Compressors," *Journal of Turbomachinery*, Vol. 129, (2), April 2007, pp. 412–420.

[114] Gottfried, D. A., and Fleeter, S., "Aerodynamic Damping Predictions in Turbomachines Using a Coupled Fluid-Structure Model," *Journal of Propulsion and Power*, Vol. 21, (2), March-April 2005, pp. 327–334.

[115] Ramakrishnan, K., Lawless, P. B., and Fleeter, S., "Finite Element Simulation of Blade Row Viscous Interactions: Vane Vibratory Stress Prediction," *Journal of Propulsion and Power*, Vol. 23, (1), January-February 2007, pp. 212–220.

[116] Datta, A., Nixon, M. and Chopra, I., "Review of Rotor Loads Prediction with the Emergence of Rotorcraft CFD," *Journal of the American Helicopter Society*, Vol. 52, (4), October 2007, pp. 287–217.

[117] Strawn, R. C., Caradonna, F. X. and Duque, E. P. N., "30 Years of Rotorcraft Computational Fluid Dynamics Research and Development," *Journal of the American Helicopter Society*, Vol. 51, (1), January 2006, pp.5–21.

[118] Hodges, D. H., and Dowell, E. H., "Nonlinear Equations of Motion for the Elastic Bending and Torsion of Twisted Nonuniform Rotor Blades," NASA TN D-7818, December 1974.

[119] Ormiston, R. A., Hodges, D. H., and Peters, D. A., "On the Nonlinear Deformation Geometry of Euler-Bernoulli Beams," NASA Technical Paper 1566, 1980.

[120] Kvaternik, Raymond G., Kaza, Krishna R. V., Nonlinear Curvature Expressions for Combined Flapwise Bending, Chordwise Bending, Torsion, and Extension of Twisted Rotor Blades, NASA TM X-73, 997, 1976.

[121] Rosen, A. and Friedmann, P.P., "Nonlinear Equations of Equilibrium for Elastic Helicopter or Wind Turbine Blades Undergoing Moderate Deformation," Report UCLA-ENG 7718, University of California at Los Angeles, June 1977 (also NASA CR-159478, 1978).

[122] Hodges, D.H., "Geometrically exact, intrinsic theory for dynamics of curved and twisted anisotropic beams," *AIAA Journal*, Vol. 41, (6), June, 2003, pp. 1131–1137, see also, "Erratum: Geometrically exact, intrinsic theory for dynamics of curved and twisted anisotropic beams," *AIAA Journal*, Vol. 42, (7), July, 2004, pp. 1500–1500.

[123] Johnson, W., "Rotorcraft Dynamics Models for a Comprehensive Analysis," American Helicopter Society 54th Annual Forum Proceedings, Washington D.C., May 20–22, 1998.

[124] Friedmann, P. P., "Rotary-Wing Aeroelasticity: Current Status and Future Trends," *AIAA Journal*, Vol. 42, (10), 2004, pp. 1953–1972.

[125] Cesnik, C. E. S., "VABS: A New Concept for Composite Rotor Blade Cross-Sectional Modeling," *Journal of the American Helicopter Society*, Vol. 42, (1), Jan 1997, pp. 27–38.

[126] Hodges, D. H., Atilgan, A. R., Cesnik, C. E. S., Fulton, M. V., "On a Simplified Strain Energy Function for Geometrically Nonlinear Behavior of Anisotropic Beams,", *Composites Engineering*, Vol. 2, (5–7), 1992, pp. 513–526.

[127] Smith, E. C. and Chopra, I., "Aeroelastic Response, Loads, and Stability of a Composite Rotor in Forward Flight," *AIAA Journal*, Vol. 31, (7), July 1993, pp. 1265–1273.

[128] Berdichevsky, V. L, Armanios, E. A., and Badir, A. M., "Theory of Anisotropic Thin-Walled Closed-Section Beams," *Composites Engineering*, Vol. 2, (5–7), 1992, pp. 411–432.

[129] Volovoi, V. V. and Hodges, D. H., "Theory of Anisotropic Thin-Walled Beams," *Journal of Applied Mechanics*, Vol. 67, (3), 2000, pp. 453–459.

[130] Kosmatka, J. B., "Extension-Bend-Twist Coupling Behavior of Nonhomogeneous Anisotropic Beams with Initial Twist," *AIAA Journal*, vol. 30, (2), 1992, pp. 519–527.

[131] Yu, W., Hodges, D. H., Volovoi, V. V. and Cesnik, C. E. S., "On Timoshenko-Like Modeling of Initially Curved and Twisted Composite Beams," *International Journal of Solids and Structures*, Vol. 39, (19), 2002, pp. 5101–5121.

[132] Gandhi, F., and Chopra, I., "Analysis of Bearingless Main Rotor Aeroelasticity Using an Improved Time Domain Nonlinear Elastomeric Damper Model," *Journal of the American Helicopter Society*, Vol. 41, (3), July 1996, pp. 267–277.

[133] Smith, E., Govindswamy, K., Beale, M. R., and Lesieutre, G., "Formulation, Validation and Application of a Finite Element Model for Elastomeric Lag Dampers," *Journal of the American Helicopter Society*, Vol. 41, (3), July 1996, pp. 247–256.

[134] Bauchau, O. A., Kang, N. K., "A Multibody Formulation for Helicopter Structural Dynamic Analysis," *Journal of the American Helicopter Society*, Vol. 38, (2), April 1993, pp. 3–14.

[135] Hodges, D. H., Hopkins, A. S., Kunz, D. L., and Hinnant, H. E., "Introduction to GRASP-General Rotorcraft Aeromechanical Stability Program-A Modern Approach to Rotorcraft Modeling," *Journal of the American Helicopter Society*, Vol. 32, (2), April 1987, pp. 78–90.

[136] Bauchau, O. A., Bottaso, C. L., and Nikishkov, Y. G., "Modeling Rotorcraft Dynamics with Finite Element Multibody Procedures," *Mathematical and Computer Modeling*, Vol. 33, (10), May 2001, pp. 1113–1137.

[137] Ghiringhelli, G. L., Masarati, P., Mantegazza, P., and Nixon, M. W., "Multi-body Analysis of Tiltrotor Configuration," *Nonlinear Dynamics*, Vol. 19, (4), August 1999, pp. 333–357.

[138] Gerstenberger, W., and Wood, E. R., "Analysis of Helicopter Aeroelastic Characteristics in High-Speed Flight," *AIAA Journal*, Vol. 1, (10), 1963, pp. 2366–2381.

[139] Staley, J. A., and Sciarra, J. J., "Coupled Rotor/Airframe Vibration Prediction Methods," *Rotorcraft Dynamics*, NASA SP-352, 1974, pp. 81–90.

[140] Hohenemser, K. H., and Yin, S. K., "The Role of Rotor Impedance in the Vibration Analysis of Rotorcraft," *Vertica*, Vol. 3, (3,4), 1979, pp. 187–204.

[141] Gable, R., and Sankewitsch, V., "Rotor-Fuselage Coupling by Impedance," American Helicopter Society 42nd Annual Forum Proceedings, Washington D. C., June 2-5, 1986.

[142] Dompka, R. V., and Corrigan, J. J., "AH-1G Flight Vibration Correlation Using NASTRAN and the C81 Rotor/Fuselage Coupled Analysis," American Helicopter Society 42nd Annual Forum Proceedings, Washington D. C., June 2-5, 1986.

[143] Kvaternik, R. G., "The NASA/industry Design Analysis Methods for Vibrations (DAMVIBS) Program: A Government Overview," Paper 1992-2200, AIAA/ASME/ASCE/AHS/ASC Structures, Structural Dynamics and Materials Conference, 33rd, Dallas, TX, Apr 13-15, 1992.

[144] Cronkhite, J. D., "The NASA/industry Design Analysis Methods for Vibrations (DAMVIBS) Program - Bell Helicopter Textron Accomplishments," Paper AIAA 1992-2201, AIAA/ASME/ASCE/AHS/ASC Structures, Structural Dynamics and Materials Conference, 33rd, Dallas, TX, Apr 13-15, 1992.

[145] Gabel, R., Lang, P., and Reed, D., "The NASA/industry Design Analysis Methods for Vibrations (DAMVIBS) Program - Boeing Helicopters Airframe Finite Element Modeling," Paper AIAA 1992-2202, AIAA/ASME/ASCE/AHS/ASC Structures, Structural Dynamics and Materials Conference, 33rd, Dallas, TX, Apr 13-15, 1992.

[146] Toossi, M., Weisenburger, R., and Hashemi-Kia, M., "The NASA/industry Design Analysis Methods for Vibrations (DAMVIBS) Program - McDonnell Douglas Helicopter Company Achievements," Paper AIAA 1992-2203, AIAA/ASME/ASCE/AHS/ASC Structures, Structural Dynamics and Materials Conference, 33rd, Dallas, TX, Apr 13-15, 1992.

[147] Twomey, W. J., "The NASA/industry Design Analysis Methods for Vibrations (DAMVIBS) Program - Sikorsky Aircraft - Advances Toward Interacting With The Airframe Design Process," Paper AIAA 1992-2204, AIAA/ASME/ASCE/AHS/ASC Structures, Structural Dynamics and Materials Conference, 33rd, Dallas, TX, Apr 13-15, 1992.

[148] Kvaternik, R. G., Bartlett, F. D. Jr., and Cline, J. H., "A Summary of Recent NASA/Army Contributions to Rotorcraft Vibration and Structural Dynamics Technology," NASA CP-2495, February 1988.

[149] Stephens, W. B., and Peters, D. A., "Rotor-Body Coupling Revisited," *Journal of the American Helicopter Society*, Vol. 32, (1), 1987, pp. 68–72.

[150] Vellaichamy, S., and Chopra, I., "Effect of Modeling Techniques in the Coupled Rotor-Body Vibration Analysis," Paper AIAA 93-1360, April 1993.

[151] Chiu, T., and Friedmann, P. P., "A Coupled Helicopter Rotor/Fuselage Aeroelastic Response Model for ACSR," Paper AIAA 95-1126, April 1995.

[152] Cribbs, R.C., Friedmann, P.P., and Chiu, T., "Coupled Helicopter Rotor/Flexible Fuselage Aeroelastic Model for Control of Structural Response," *AIAA Journal*, Vol. 38, (10), Oct 2000.

[153] Yeo, H., Chopra, I., "Coupled Rotor/Fuselage Vibration Analysis Using Detailed 3-D Airframe Models," *Mathematical and Computer Modelling* 33 (2001) pp. 1035-1054.

[154] Mao, Y. and Chopra, I., "Vibration Prediction for Rotor System with Faults Using Coupled Rotor-Fuselage Model," *Journal of Aircraft*, Vol. 41, (2), March-April 2004, pp. 348–358.

[155] Bauchau, O. A., Rodriguez, J., Chen, S., "Coupled Rotor-Fuselage Analysis with Finite Motions Using Component Mode Synthesis", *Journal of the American Helicopter Society*, Vol. 49, No. 2, April 2004, pp. 201-211.

[156] Tung, C., Cardonna, F.X., and Johnson, W.R., "The Prediction of Transonic Flows on an Advancing Rotor," *Journal of the American Helicopter Society*, Vol. 31, (3), July 1986, pp. 4–9.

[157] Strawn, R.C. and Tung, C., "Conservative Full Potential Model for Unsteady Transonic Rotor Flows," *AIAA Journal*, Vol. 25, (2), February 1987 pp. 193–198.

[158] Kim, K. C., Desopper, A. and Chopra, I.,"Blade Response Calculations Using Three-Dimensional Aerodynamic Modeling," *Journal of American Helicopter Society*, Vol. 36, (1), January 1991, pp. 68–77.

[159] Beaumier, P., "A Coupling Procedure Between a Rotor Dynamics Code and a 3D Unsteady Full Potential Code," American Helicopter Society Aeromechanics Specialists' Conference, San Francisco, CA, January 19–21, 1994.

[160] Bousman, W. G., Young, C., Toulmay, F., Gilbert, N. E., Strawn, R. C., Miller, J. V., Maier, T. H., Costes, M. and Beaumier P., "A Comparison of Lifting-Line and CFD Methods with Flight Test Data from a Research Puma Helicopter," NASA TM 110421 USAATCOM TP 96-A-008, October 1996.

[161] Philippe, J. J., "Survey on ONERA Code Developments and Validation Studies for Multidisciplinary Research on Rotor Aeromechanics," American Helicopter Society Aeromechanics Specialists' Conference, San Francisco, CA, January 19–21, 1994.

[162] Datta, A., and Chopra, I, "Validation of Structural and Aerodynamic Modeling using UH-60A Airloads Program Data," *Journal of the American Helicopter Society*, Vol. 51, (1), January 2006, pp. 43–58.

[163] Datta, A., Sitaraman, J., Chopra., I, and Baeder, J., "CFD/CSD prediction of rotor vibratory loads in high speed flight," in press, *Journal of Aircraft*, Vol. 43, (6), Nov.-Dec. 2006, pp. 1698–1709.

[164] Potsdam, M., Yeo, H., Johnson, W., "Rotor Airloads Prediction Using Loose Aerodynamic/Structural Coupling," *Journal of Aircraft*, Vol. 43, (3), May/June, 2006, pp. 732–742.

[165] Sitaraman, J. and Baeder, J., "Field Velocity Approach and Geometric Conservation Law for Unsteady Flow Simulations," *AIAA Journal*, Vol. 44, (9), September 2006, pp. 2084–2094.

[166] Datta, A. and Chopra, I., "Prediction of UH-60A Dynamic Stall Loads in High Altitude Level Flight using CFD/CSD Coupling," American Helicopter Society 61st Annual Forum Proceedings, Grapevine, Texas, June 1-3, 2005.

[167] Duraisamy, K. and Baeder, J. D., "High Resolution Wake Capturing Methodology for Hovering Rotors," *Journal of the American Helicopter Society*, Vol. 52, (2), April 2007, pp.110–122.

[168] Sitaraman, J., Datta, A., Baeder, J., and Chopra, I., "Prediction of Rotor aerodynamic and Structural Loads at Three Critical Level Flight Conditions," 31st European Rotorcraft Forum, Florence, Italy, Sep. 12-15, 2005.

[169] Datta, A. and Chopra, I., "Prediction of UH-60 Main Rotor Structural Loads using CFD/Comprehensive Analysis Coupling," 32nd European Rotorcraft Forum, Maastricht, The Netherlands, September 12–14, 2006.

[170] Lim, J. W., Nygaard, T. A., Strawn, R., and Potsdam, M., "Blade-Vortex Interaction Airloads Prediction Using Coupled Computational Fluid and Structural Dynamics," *Journal of the American Helicopter Society*, Vol. 52, (4), October 2007, pp.318–328.

[171] Servera, G., Beaumier, P., and Costes, M. "A Weak Coupling Method between the Dynamics Code Host and the 3D Unsteady Euler Code Waves," 26th European Rotorcraft Forum, The Hague, Netherlands, September 14–16, 2000.

[172] Altmikus, A. R. M., Wagner, S., Beaumier, P., and Servera, G., "A Comparison : Weak versus Strong Modular Coupling for Trimmed Aeroelastic Rotor Simulation," American Helicopter Society 58th Annual Forum, Montreal, Quebec, June 2002.

[173] Pomin, H. and Wagner, S. "Aeroelastic Analysis of Helicopter Rotor Blades on Deformable Chimera Grids," *Journal of Aircraft*, Vol. 41, (3), May-June 2004, pp. 577-584.

[174] Pahlke, K. and Van Der Wall, B., "Chimera simulations of multibladed rotors in high-speed forward flight with weak fluid-structure-coupling," *Aerospace Science and Technology*, Vol. 9, (5), 2005, pp. 379–389.

[175] van der Weide, E., Kalitzin, G., Schluter, J., and Alonso, J. J., "Unsteady Turbomachinery Computations Using Massively Parallel Platforms," Paper AIAA 2006-421, AIAA Aerospace Sciences Meeting and Exhibit, 44th, Reno, NV, January 9-12, 2006.

[176] Gopalan, G., Sitaraman, J., Baeder, J. D., and Schmitz, F. H., "Aerodynamic and Aeroacoustic Prediction Methodologies with Application to the HART II Model Rotor," Presented at the American Helicopter Society 62nd Annual Forum, Phoenix, Arizona, May 9-11, 2006. Not part of proceedings, available only upon request.

[177] Duque, E., Sankar, L., Menon, S., Bauchau, O., Ruffin, S., Smith, M., Ahuja, K., Brentner, K., Long, L., Morris, P., and Gandhi, F., "Revolutionary Physics-Based Design Tools for Quiet Helicopters," Paper AIAA 2006-1068, AIAA Aerospace Sciences Meeting and Exhibit, Reno, NV, January 9-12, 2006.

[178] Shelton, A. B., Braman, K., Smith, M. J., and Menon, S., "Improved Turbulence Modeling For Rotorcraft," Presented at the American Helicopter Society 62nd Annual Forum, Phoenix, Arizona, May 9-11, 2006. Not part of proceedings, available only upon request.

[179] Jain, R. K., Ramakrishnan, S. V., and Chen, C., "Enhancement of WIND-US for Helicopter Rotor Flow Simulations," Paper AIAA 2006-3373, AIAA Fluid Dynamics Conference and Exhibit, 36th, San Francisco, CA, June 5-8, 2006.

[180] Bauchau, O., A. and Ahmad, J., U., " Advanced CFD and CSD Methods for Multidisciplinary Applications of Rotorcraft Problems," AIAA 6th Symposium on Multidisciplinary Analysis and Optimization, Seattle, WA, September 4–6, 1996.

[181] Bhagwat, M. J., Ormiston, R. A., Saberi, H. A. and Xin, H., "Application of CFD/CSD Coupling for Analysis of Rotorcraft Airloads and Blade Loads in Maneuvering Flight," American Helicopter Society 63rd Annual Forum Proceedings, Virginia Beach, VA, May 1-3, 2007.